The freshwater composition of the Fram Strait outflow derived from a decade of tracer measurements

Paul A. Dodd,[1] Benjamin Rabe,[2] Edmond Hansen,[1] Eva Falck,[3] Andreas Mackensen,[2] Eelco Rohling,[4] Colin Stedmon,[5] and Svein Kristiansen[6]

Received 1 March 2012; revised 10 August 2012; accepted 29 August 2012; published 6 November 2012.

[1] The composition of the Fram Strait freshwater outflow is investigated by comparing 10 sections of concurrent salinity, δ^{18}O, nitrate and phosphate measurements collected between 1997 and 2011. The largest inventories of net sea ice meltwater are found in 2009, 2010 and 2011. The 2009–2011 sections are also the first to show positive fractions of sea ice meltwater at the surface near the core of the EGC. Sections from September 2009–2011 show an increased input of sea ice meltwater at the surface relative to older September sections. This suggests that more sea ice now melts back into the surface in late summer than previously. Comparison of April, July and September sections reveals seasonal variations in the inventory of positive sea ice meltwater, with maximum inventories in September sections. The time series of sections reveals a strong anti-correlation between meteoric water and net sea ice meltwater inventories, suggesting that meteoric water and brine may be delivered to Fram Strait together from a common source. We find that the freshwater outflow at Fram Strait exhibits a similar meteoric water to net sea ice meltwater ratio as the central Arctic Ocean and Siberian shelves, suggesting that much of the sea ice meltwater and meteoric water at Fram Strait may originate from these regions. However, we also find that the ratio of meteoric water to sea ice meltwater inventories at Fram Strait is decreasing with time, due to an increased surface input of sea ice meltwater in recent sections.

Citation: Dodd, P. A., B. Rabe, E. Hansen, E. Falck, A. Mackensen, E. Rohling, C. Stedmon, and S. Kristiansen (2012), The freshwater composition of the Fram Strait outflow derived from a decade of tracer measurements, *J. Geophys. Res.*, *117*, C11005, doi:10.1029/2012JC008011.

1. Introduction

1.1. The Fram Strait Outflow and the MOC

[2] The Arctic Ocean exports low-density freshwater at the surface, which is transported to the North Atlantic, Nordic and Labrador Seas where it has the potential to slow the MOC by reducing the formation of dense water [e.g., *Arzel et al.*, 2008]. Freshwater budgets such as those from *Aagard and Carmack* [1989] and *Serreze et al.* [2006] suggest that the freshwater outflow from the Arctic Ocean has three principle components: River input from Eurasian and North American rivers; sea ice formed in the Arctic Ocean; and relatively fresh Pacific seawater, which enters the Arctic Ocean through the Bering Strait (Figure 1). The input of glacial ice meltwater discharge from Greenland (estimated by studies such as *Rignot and Kanagaratnam* [2006]) is an order of magnitude smaller than the volume of river input. The volume of precipitation that enters the Arctic Ocean directly is not well known due to the difficulty of maintaining a network of precipitation gauges in the Arctic Ocean. However, the surface area of the Arctic Ocean is small compared with the combined drainage basin area of rivers flowing into it.

1.2. Increasing Freshwater Inputs to the Arctic Ocean

[3] A number of studies suggest that the rate at which freshwater is supplied to the Arctic Ocean has been increasing since the 1960s, for example: *Peterson et al.* [2002], *Box et al.* [2004], and *Overeem and Syvitski* [2010]. Concurrently, observations suggest that the freshwater inventory is increasing in the Arctic Ocean [*Rabe et al.*, 2011; *Giles et al.*, 2012].

[4] Modeling studies such as *Wu et al.* [2005] estimate that river input to the Arctic Ocean has increased at a mean rate of 1.82 ± 0.6 km^3 yr^{-1} since 1930s, relative to a 3150 km^3 yr^{-1} mean. The estimate of *Wu et al.* [2005] is consistent with the observational discharge study by *Peterson et al.* [2002], who

[1] Norwegian Polar Institute, Tromsø, Norway.
[2] Alfred Wegener Institute for Polar and Marine Research, Bremerhaven, Germany.
[3] The University Centre in Svalbard, Longyearbyen, Norway.
[4] National Oceanography Centre, Southampton, Southampton, UK.
[5] National Institute for Aquatic Resources, Technical University of Denmark, Charlottenlund, Denmark.
[6] Department of Arctic and Marine Biology, University of Tromsø, Tromsø, Norway.

Corresponding author: P. A. Dodd, Norwegian Polar Institute, Tromsø NO-9296, Norway. (paul.dodd@npolar.no)

Published in 2012 by the American Geophysical Union.

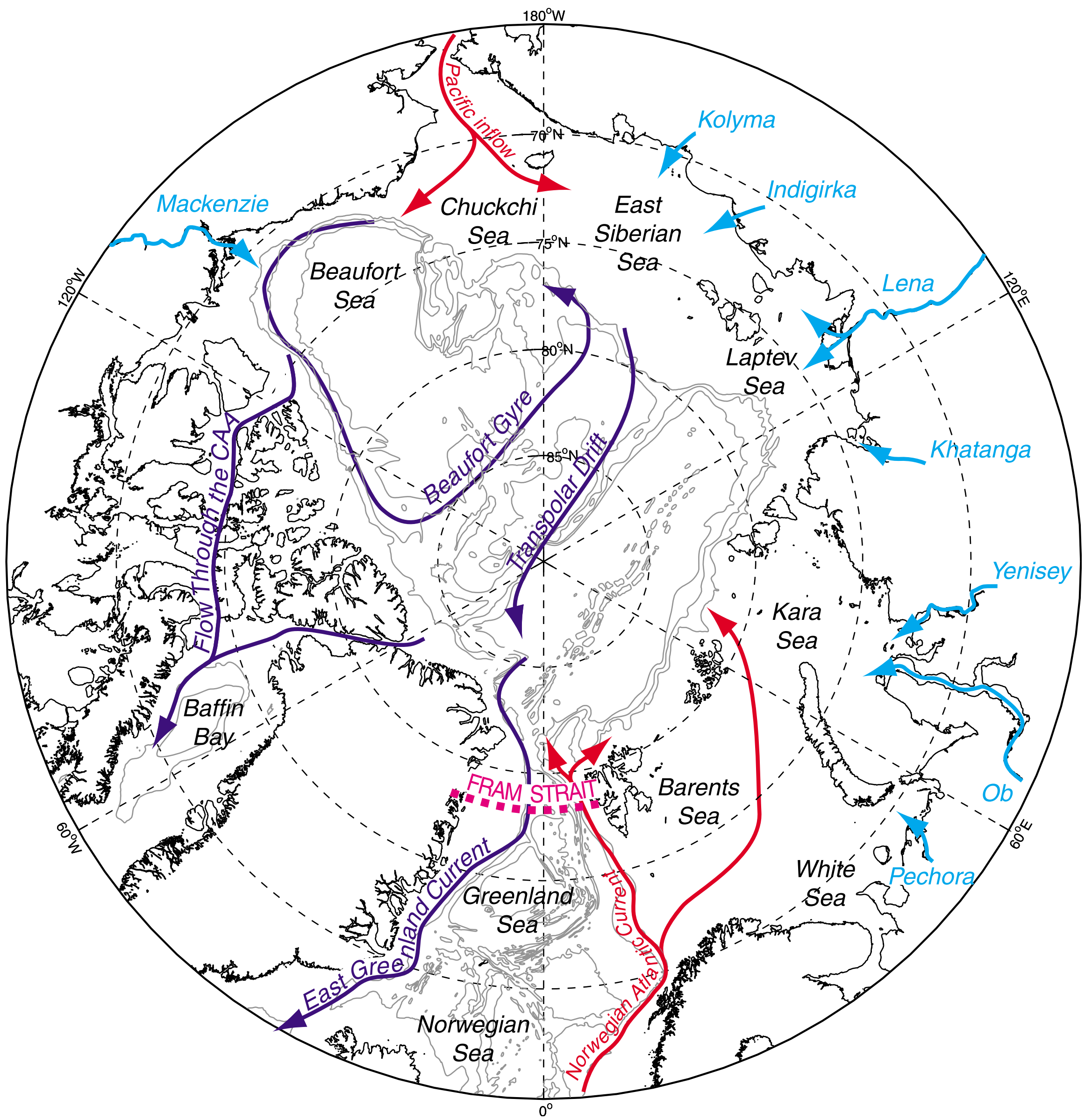

Figure 1. Schematic map showing the surface circulation of the Arctic Ocean and the repeated Fram Strait section. Inflowing currents are shown in red, outflowing currents in dark blue and major rivers in light blue. Bathymetric contours are drawn at 1000 m intervals.

calculate an increase of 2.0 ± 0.7 km^3 yr^{-1} using archived observations, and with *New et al.* [2001], who observe sufficient increases in precipitation to drive the additional discharge.

[5] The declining extent of Arctic sea ice may also represent a source of freshwater to the Arctic Ocean. The long term reduction in Arctic sea ice extent of 3% per decade determined from satellite measurements by *Parkinson et al.* [1999] and *Parkinson and Calivari* [2002] has recently accelerated to rates of 9–10% per decade in the perennial sea ice cover [e.g., *Stroeve et al.*, 2007]. More recently *Comiso et al.* [2008] have observed that the reduction of the entire ice extent has accelerated to rates of 10–11% per decade. In terms of volume, *Kwok et al.* [2009] determined that the reduction in the perennial sea ice extent accounted for most of the net volume reduction between 2003 and 2008, based on an analysis of freeboard-resolving ICESat data.

1.3. The Composition of the Fram Strait Freshwater Outflow

[6] Between 1997 and 2005 *Meredith et al.* [2001] and *Rabe et al.* [2009] collected four sections of concurrent salinity and δ^{18}O measurements across Fram Strait and separated the net freshwater inventory into meteoric water and net sea ice meltwater fractions.

[7] The term meteoric water includes: precipitation that entered the ocean directly, runoff, glacial ice meltwater and snow that entered the ocean after residing on sea ice. Meteoric water fractions are typically double the net freshwater fractions that would be determined using salinity measurements alone. This is because without the benefit of suitable tracer measurements, brine rejected during sea ice formation obscures some of the meteoric water input. Positive fractions

Table 1. Cruises During Which the Tracer Samples Used in This Study Were Collected

Cruise Number	Year	Month	$\delta^{18}O^a$	N:P[a]	Platform	Cruise	DOI
1	1997	September	⋆	-	R/V Polarstern	ArkXIII	10.1594/PANGAEA.742654
2	1998	September	⋆	⋆	R/V Polarstern	ArkXIV	10.1594/PANGAEA.759130
3	2004	August	⋆	⋆	R/V Polarstern	ArkXXI	10.1594/PANGAEA.742660
4	2005	August	⋆	⋆	R/V Polarstern	ArkXXII	10.1594/PANGAEA.742621
5	2008	April	⋆	⋆	K/V Svalbard	iAOOS 2008	(no DOI)
6	2008	July	⋆	⋆	R/V Polarstern	ArkXV	10.1594/PANGAEA.733424
7	2008	September	⋆	-	R/V Lance	FS 2008	(no DOI)
8	2009	September	⋆	⋆	R/V Lance	FS 2009	(no DOI)
9	2010	September	⋆	⋆	R/V Lance	FS 2010	(no DOI)
10	2011	September	⋆	⋆	R/V Lance	FS 2011	(no DOI)

[a]A star indicates that samples were collected. A dash indicates that samples were not collected.

of sea ice meltwater are not generally found in Fram Strait. Rather, the net formation of sea ice in the Arctic Ocean leaves negative fractions of sea ice meltwater in the outflow [*Meredith et al.*, 2001].

[8] The fraction of Pacific water at Fram Strait was observed approximately biennially between 1988 and 2006 [*Falck et al.*, 2008]. The series of sections presented revealed large variations between surface maxima of more than 80% to minima of around 40% varying with a periodicity of 6–10 years.

1.4. This Study

[9] In this study we collate repeated sections of concurrent salinity, δ^{18}O and nitrate and phosphate measurements collected between 1997 and 2011. The repeated sections allow direct comparison of the freshwater composition in different years. We investigate how different freshwater fractions contribute to the overall freshwater inventory and how the composition of freshwater flowing out of the Arctic Ocean through Fram Strait has varied during the last decade.

2. Data

2.1. Sample Collection

[10] CTD and tracer sections close to 78 50′N were completed during the course of 10 cruises to Fram Strait (Table 1). The latitude 78 50′N is indicated by a dashed magenta line on Figure 1. The location of stations and the extent of sampling varied between cruises; station positions and sampling depths for each cruise are shown on Figure 2.

[11] Samples for laboratory salinity and δ^{18}O measurement were collected on all cruises. Dissolved nitrate and phosphate concentration samples were collected on all cruises except those in September 1997 and September 2008.

[12] In all cases water samples were collected using rosette water samplers equipped with Niskin type bottles. Separate water samples for salinity, δ^{18}O and nutrient analyses were drawn from Niskin bottles immediately after the CTD package was secured in a heated area. West of 11 W in April 2008 samples were collected from ice floes (accessed by helicopter) using a single Niskin bottle closed with a brass messenger. Samples were drawn from these Niskin bottles in the open, but in fair weather.

[13] Salinity samples were analyzed at sea using either a Guildline 8400 salinometer (accuracy ca. ±0.002) or Guildline Portasal salinometer (accuracy ca. ±0.003). δ^{18}O samples were analyzed ashore by standard equilibration with carbon dioxide following the procedure described by *Epstein and Mayeda* [1953], but using automated analysis lines. Accuracy was estimated to be better than ±0.04‰ relative to Vienna standard mean ocean water (VSMOW). δ^{18}O samples were analyzed at: The University of East Anglia, UK (1997, 1998), the Alfred Wegener Institute, Bremerhaven, Germany (2004, 2005, July 2008), the British Geological Survey, UK (April 2008, September 2008, 2010) the National Oceanography Centre, Southampton, UK (2009) and the G.G. Hatch Stable Isotope Laboratory, University of Ottawa, Canada (2011).

[14] Dissolved nutrient samples were analyzed using automated analysis lines according to the WOCE protocol [*Gordon et al.*, 1993] to an accuracy of ca. ±1%. Samples that were not analyzed at sea were frozen at $<-20°$C after collection and analyzed ashore. Dissolved nutrient samples were analyzed at: The Alfred Wegener Institute, Bremerhaven, Germany (August 2004), The University in Tromsø, Norway (April 2008), Aarhus University, Roskilde, Denmark (2009, 2010, 2011), at sea (1998, 2005, September 2008).

2.2. δ^{18}O and Salinity Measurements

[15] Figure 3 shows the δ^{18}O and salinity measurements collated in this study. The solid black line on Figure 3 joining Atlantic water ($\delta^{18}O = 0.3$, S = 34.9) and meteoric water ($\delta^{18}O = -18.4$, S = 0), is the meteoric water -Atlantic water (MW-AW) mixing line. In the absence of sea ice melt or formation processes all points would lie very close to this line. Sea ice formation moves points to the right of the MW-AW mixing line because it significantly increases the salinity of seawater while only slightly lowering the δ^{18}O. The addition of sea ice meltwater moves points to the left of the MW-AW mixing line. Most of the points on Figure 3 lie to the right of the MW-AW mixing line due to the net formation of sea ice which occurs in the Arctic Ocean.

[16] The addition of Pacific seawater in samples moves points downwards along the MW-AW mixing line and very slightly to the right. Pacific seawater has a slightly lower salinity and δ^{18}O ($\delta^{18}O = -1.3$, S = 32.0) than Atlantic seawater ($\delta^{18}O = 0.3$, S = 34.9). However, the amount of Pacific seawater in samples cannot be quantitatively determined without using an additional tracer. Most of the points on Figure 3 lie along one of three following limbs.

2.2.1. Limb A

[17] Samples lying along limb A are found across all longitudes in Fram Strait and typically between 25 and 300 dbar (Figure 4, top row). Note that these samples are less common in the very surface (0–50 dbar layer). The lack of samples below 300 dbar is due to a lack of deep sampling and

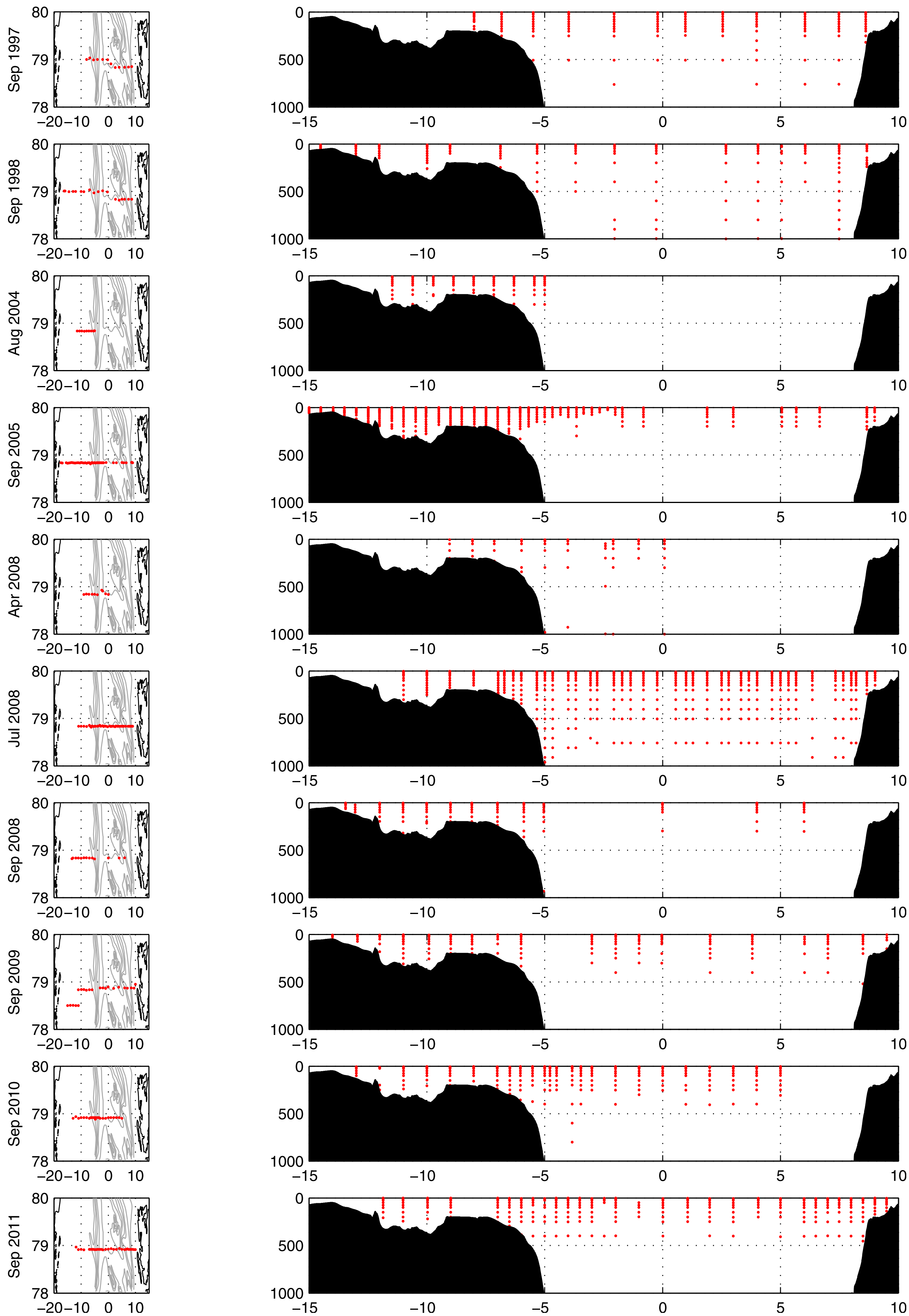

Figure 2. Maps and sections showing sampling locations in terms of longitude and pressure (dbar) during each cruise. Bathymetric contours are drawn at 500 m intervals.

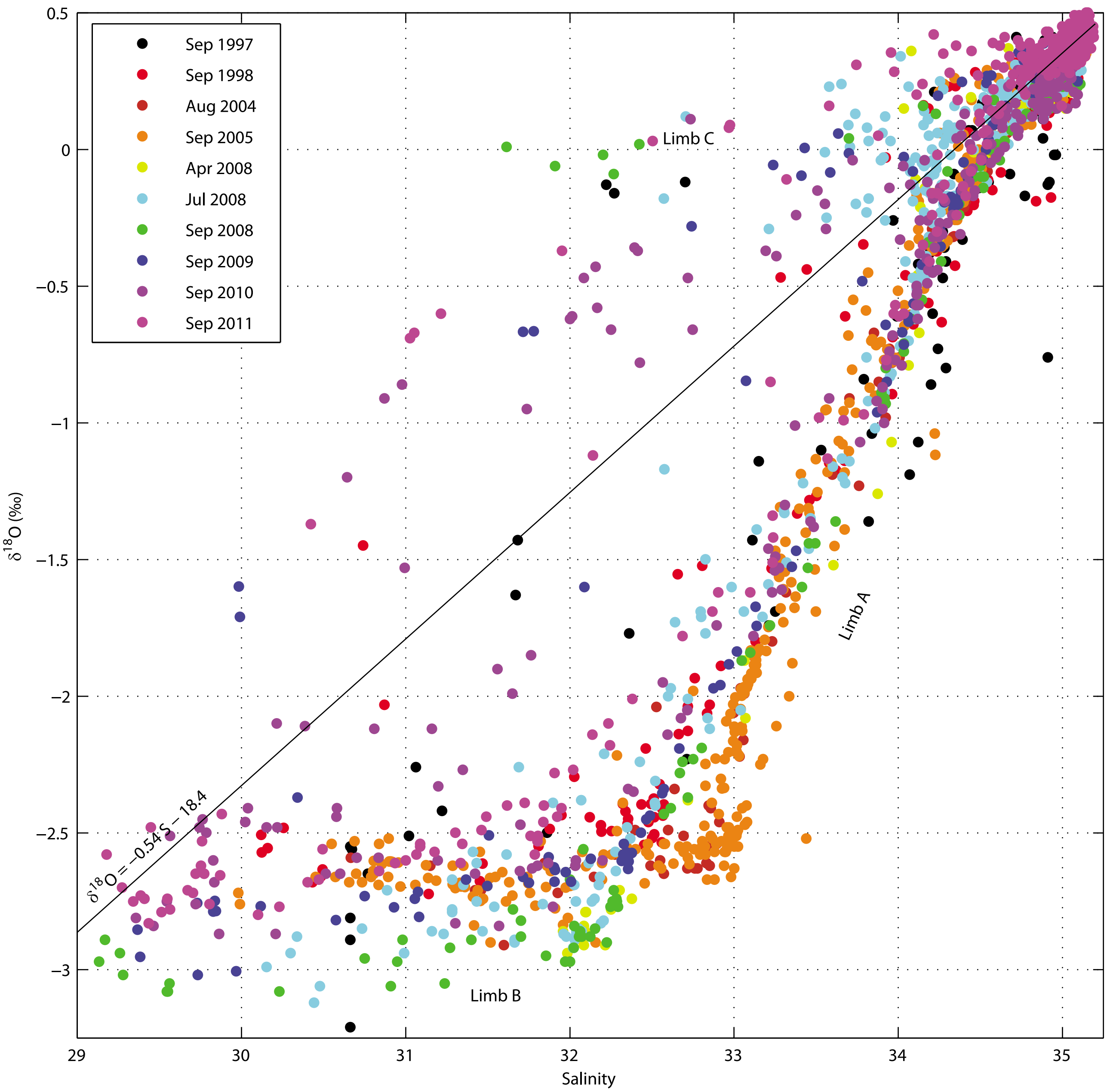

Figure 3. Samples from each cruise in δ^{18}O - salinity space. The solid black line is the meteoric water - Atlantic seawater mixing line.

not due to a sudden change in δ^{18}O or salinity values at 300 dbar. The gradient of limb A is defined by the proportions of net sea ice meltwater (typically negative), meteoric water and (to a lesser extent) Pacific seawater present in polar surface water exiting the Arctic Ocean in the top 300 dbar.

2.2.2. Limb B

[18] Samples lying along limb B are typically found in the top 50 dbar of the water column over the East Greenland Continental Shelf from 5 to 15 W (Figure 4, middle row). These samples are from polar surface water at the surface, above the core of the East Greenland Current. They contain high fractions of meteoric water (S = 0, δ^{18}O = −18.4) and have experienced significant sea ice melting, which lowers salinity while only slightly raising δ^{18}O. Note that limb B is not present among the samples collected during the ice growth season in April 2008 because there were no significant fractions of positive sea ice meltwater in Fram Strait at that time. High positive fractions of sea ice meltwater at the surface may arise from sea ice melting in Fram Strait, but it is not possible to separate the input of meltwater at the surface occurring locally in Fram Strait from that occurring further upstream in the Arctic Ocean.

2.2.3. Limb C

[19] Samples lying along Limb C are typically found in the top 50 dbar of the water column and in eastern Fram Strait. These samples are mostly of saline water to the east of the East Greenland Current, which have acquired some sea ice

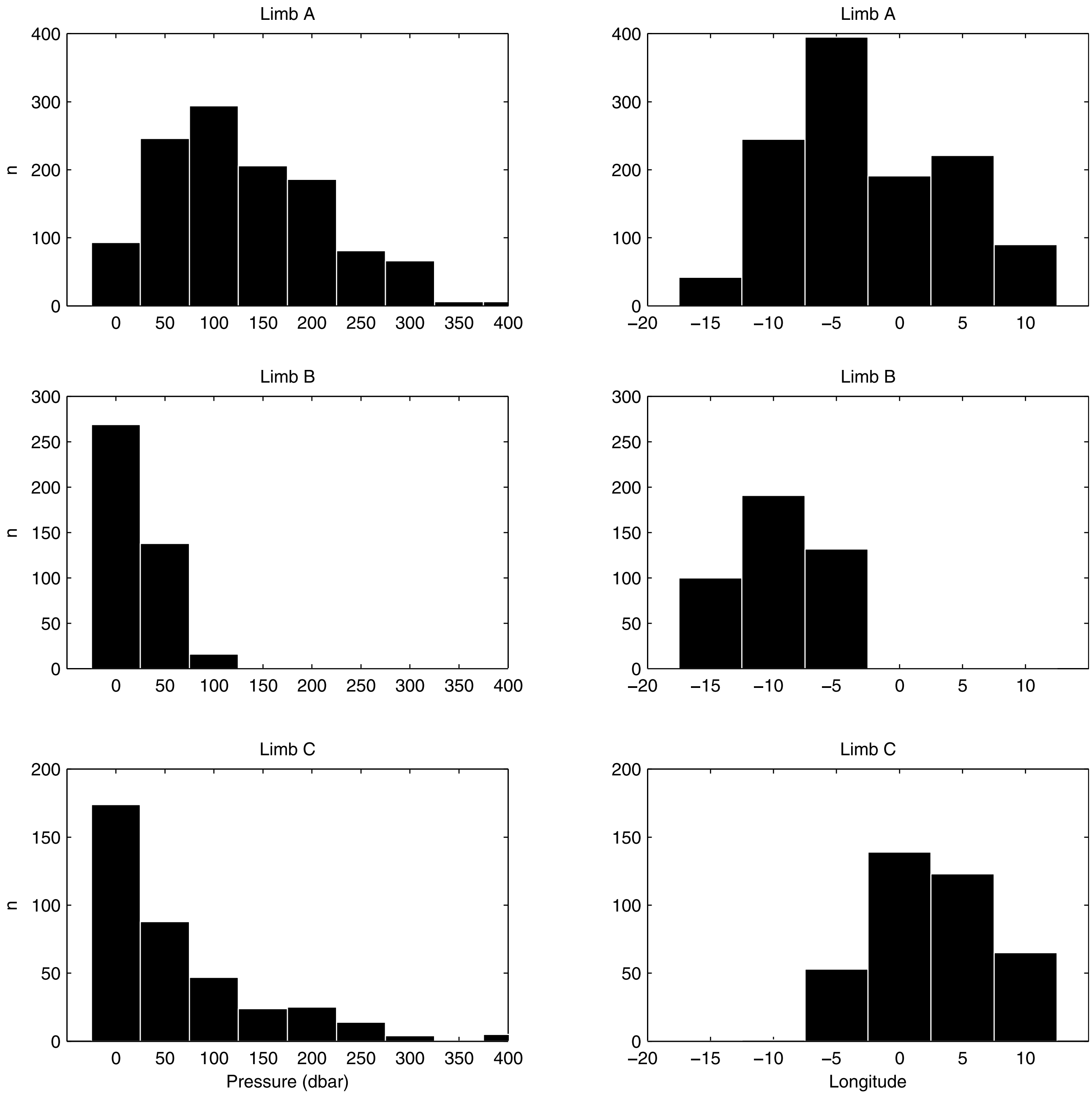

Figure 4. Histograms showing how points along each limb of Figure 3 are distributed in terms of longitude and pressure.

meltwater. The gradient of limb C is similar to that of limb B. However, samples along limb C are much more widely scattered.

3. Calculations

3.1. Mass Balance Equations

[20] To quantify the proportions of meteoric water, sea ice meltwater, Pacific seawater and Atlantic seawater in water samples we use the 4-end-member mass balance described by equations (1) to (6). Our approach follows that of *Østlund and Hut* [1984], but here we extend their 3-end-member mass balance to include a Pacific seawater end-member in a similar way to *Jones et al.* [2008a], *Yamamoto-Kawai et al.* [2008] and *Bauch et al.* [2011]:

$$P_{aw} = M_{aw}N + C_{aw} \tag{1}$$

$$P_{pw} = M_{pw}N + C_{pw} \tag{2}$$

$$f_{mw} + f_{sim} + f_{pw} + f_{aw} = 1 \tag{3}$$

$$f_{mw}S_{mw} + f_{sim}S_{sim} + f_{pw}S_{pw} + f_{aw}S_{aw} = S \tag{4}$$

Table 2. End-Members Chosen for the Identification of Freshwater Fractions in Fram Strait

Water Mass	Salinity	δ^{18}O (‰)	N:P Slope	N:P Intercept (μmoll^{-1})
Meteoric water	0	−18.4	0.053	0.170
Sea ice meltwater	4	+0.5	0.053	0.170
Pacific seawater	32.0	−1.3	0.065	0.940
Atlantic seawater	34.9	+0.3	0.053	0.170

$$f_{mw}\delta_{mw} + f_{sim}\delta_{sim} + f_{pw}\delta_{pw} + f_{aw}\delta_{aw} = \delta \tag{5}$$

$$f_{mw}P_{aw} + f_{sim}P_{aw} + f_{pw}P_{pw} + f_{aw}P_{aw} = P. \tag{6}$$

[21] f_{mw}, f_{sim}, f_{pw} and f_{aw} are the derived fractions of meteoric water, sea ice meltwater, Pacific seawater and Atlantic seawater respectively; S_{mw}, S_{sim}, S_{pw} and S_{aw} are the assigned salinities of meteoric water, sea ice meltwater, Pacific seawater and Atlantic seawater; δ_{mw}, δ_{sim}, δ_{pw} and δ_{aw} are the assigned δ^{18}O values; S, δ, P and N are the measured salinity, δ^{18}O, phosphate and nitrate values. M_{pw} and C_{pw} are the slope and intercept of the Pacific seawater N:P relationship respectively and M_{aw} and C_{aw} are the slope and intercept of the Atlantic seawater N:P relationship. Properties assigned to each end-member are listed in Table 2.

[22] δ^{18}O is used to distinguish between meteoric water and sea ice meltwater in the Arctic Ocean, because meteoric water at high latitude is strongly depleted in ^{18}O relative to VSMOW while sea ice meltwater is slightly enriched in ^{18}O relative to VSMOW. The difference is due to the negative fractionation that occurs when water evaporates as well as a small positive fraction that occurs on freezing. We refer the reader to *Østlund and Hut* [1984] and references therein for discussion of the use of δ^{18}O as a tracer for meteoric water and sea ice meltwater in the Arctic Ocean.

[23] The N:P ratio is used to distinguish Pacific seawater from Atlantic seawater in the Arctic Ocean. Pacific water contains less nitrate relative to phosphate compared with Atlantic water [*Jones et al.*, 2008a], because nitrate is removed from Pacific water by denitrification as it passes across the shallow waters of the Bering Strait and Chukchi shelf [*Jones et al.*, 1998]. Within the Arctic Ocean, nutrients tend to be removed and remineralized in approximately Redfield proportions [*Redfield et al.*, 1963]. Therefore a deficiency in nitrate relative to phosphate can be used as a quasi-conservative tracer for Pacific water within the Arctic Ocean, which has been in prolonged contact with the sediment in shallow waters. *Bauch et al.* [2011] find that the N:P ratio method tends to overestimate the fraction of Pacific-derived waters within the Transpolar Drift due to denitrification the bottom sediments of the Laptev Sea continental margin. This overestimation is one factor leading to the large uncertainty (10%) in derived Pacific water fractions.

[24] For the results of the four end-member mass balance to be valid, the salinity, δ^{18}O and N:P ratio of each end-member must be well constrained. When calculating a total freshwater fraction relative to a reference salinity, the choice of reference salinity is somewhat arbitrary. However, this is not the case when several tracers are used together in a mass balance. For example it is important that Atlantic water at the prescribed salinity actually exhibits the prescribed δ^{18}O and N:P ratio characteristics.

[25] In this study we consider the Arctic Ocean to include the Beaufort, Chukchi, East Siberian, Laptev and Kara Seas, but not the Barents Sea. All the water masses in this region are wholly derived from one or more of the following sources: Atlantic seawater, Pacific seawater, meteoric water and sea ice processes. Where freshwater has been removed from the ocean by net sea ice formation we determine a negative fraction of net sea ice meltwater.

3.2. Atlantic Seawater

[26] We use the term Atlantic seawater to describe all water entering the Arctic Ocean between Greenland and Severnaya Zemlya and prescribe a salinity of 34.9 ± 0.1. This value is chosen to approximate the flow weighted mean properties of the inflow rather than the properties of pure Atlantic water in the core of the Norwegian Atlantic Current.

[27] A δ^{18}O value for Atlantic seawater at a salinity of 34.9, was estimated by fitting a line to the δ^{18}O: salinity relationship of 125 discrete samples collected below 25 dbar (to avoid the influence of sea ice meltwater input described in section 2) in eastern Fram Strait between 1998 and 2011. The value determined at S = 34.9 was +0.3 ± 0.05‰.

[28] Analysis of samples collected in Fram Strait between 1998 and 2011 shows that the N:P ratio of Atlantic water varied between different years (Figure 5). However, the Atlantic water passing out of Fram Strait is probably a mixture of water that entered in different years. Here we determine a P intercept and slope by fitting a regression line to all N and P samples collected between 2005 and 2011. Only nitrate and phosphate measurements from samples with a potential density greater than 27.60 kgm^{-3} are included in the regression analyses because less dense samples could potentially contain a significant fraction of Pacific seawater. The end-member properties we prescribe for Atlantic water are in line with similar studies in Fram Strait such as *Jones et al.* [2008b] and *Meredith et al.* [2001].

3.3. Pacific Seawater

[29] We use the term Pacific seawater to describe all water entering the Arctic Ocean via the Bering Strait. As with the Atlantic water fraction, end-member values are chosen to represent the flow weighted mean properties of the total inflow rather than pure Pacific water in the core of the inflow.

[30] We estimate the flow weighted mean salinity of the Pacific inflow using the monthly mean transport and salinity estimates of *Woodgate and Aagard* [2005]. These are based on 14 years (1990 to 2004) of measurements from three moored instruments close to the bottom of the water column in the Bering Strait. Here we assume that the water column is homogeneous in salinity, except between May and October when we consider the mean water column salinity to be 0.75 fresher than measured bottom salinity. This approach to parameterizing seasonal salinity variations at the surface follows *Woodgate and Aagard* [2005]. The flow weighted mean salinity we determine is 32.0 ± 0.3.

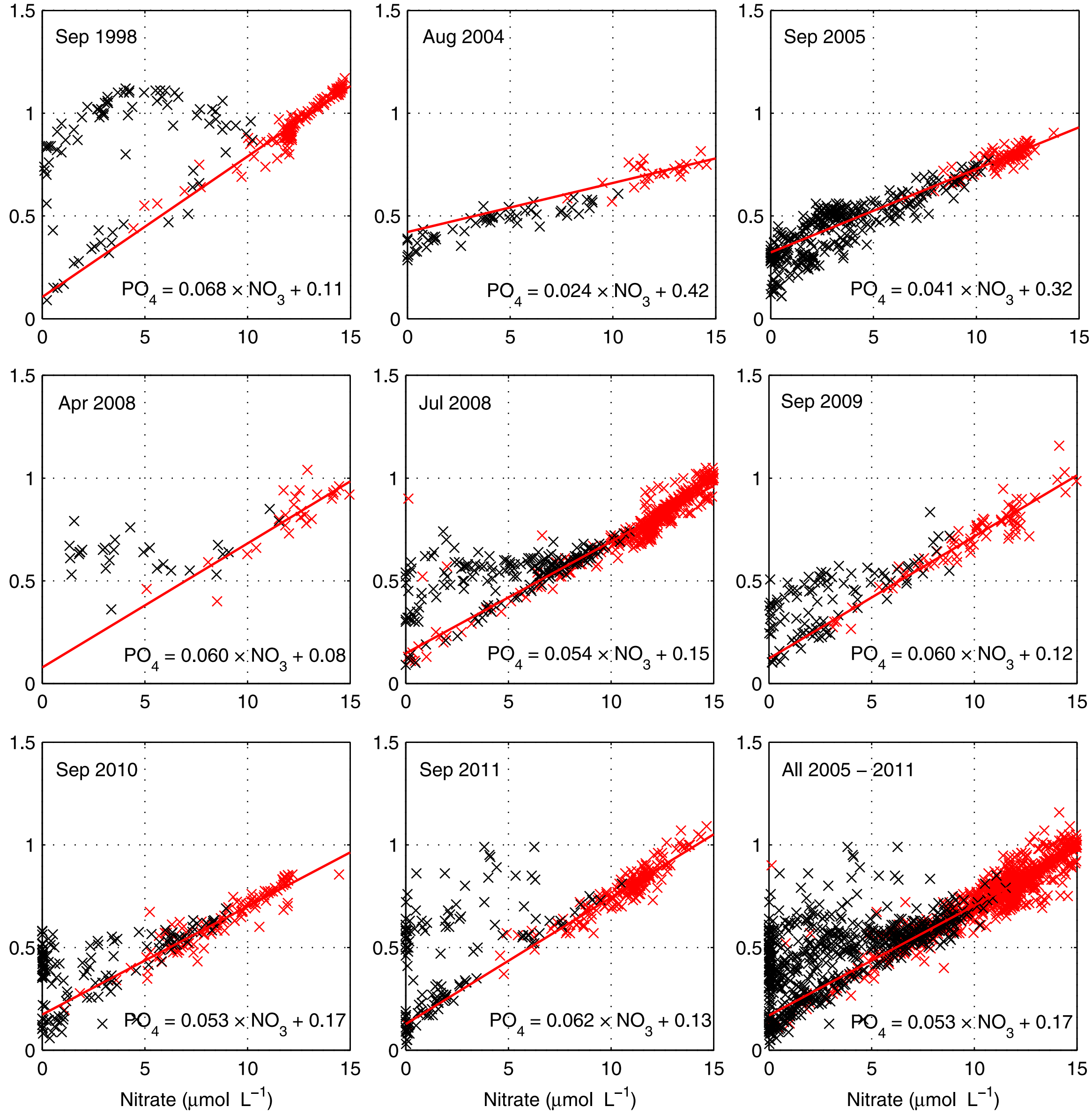

Figure 5. Nitrate and phosphate measurements collected along each cruise. Samples with a potential density greater than 27.60 kgm^{-3} are plotted in red. Only samples with a potential density greater than 27.60 kgm^{-3} are included in the regression as less dense samples could potentially contain a significant fraction of Pacific seawater. Nitrate and phosphore samples are not available for the September 1997 or September 2008 cruises.

[31] We estimate the flow weighted mean δ^{18}O of the Pacific inflow using a δ^{18}O-salinity relationship of $\delta^{18}\mathrm{O} = 0.62 \times S - 21.1$ determined for the Bering Sea shelf by *Cooper et al.* [1997] using 102 summer (June–October) samples collected between 1990 and 1993. This is the same data set used by *Ekwurzel et al.* [2001] to estimate the δ^{18}O of Pacific water. The value we determine at S = 32.0 is -1.3 ± 0.3‰.

[32] We adopt the N:P ratio of Pacific water determined by *Jones et al.* [2008a] from a transect of measurements across the Arctic Ocean collected between August and September 2005 (P = 0.0653 * N + 0.94). Due to a lack of suitable measurements we are unable to review Pacific N:P ratio end-members here. We note that *Jones et al.* [2008b] estimate a Pacific water N:P ratio of (P = 0.0675 * N + 0.82) from samples collected from the Canada basin between September and October 1997 suggesting that the N:P ratio of Pacific water may vary to a similar degree as that of Atlantic water.

[33] We use equation (7) to determine fractions of Pacific freshwater relative to Atlantic seawater. f_{pw} is the fraction of Pacific seawater and f_{pw0} is the fraction of Pacific freshwater. We prescribe reference salinities of 34.9 for Atlantic seawater and 32.0 for Pacific seawater.

$$f_{pw0} = f_{pw}(34.9 - 32.0)/34.9. \quad (7)$$

Table 3. Flow Weighted Mean $\delta^{18}O$ and Discharge Estimates for the 10 Largest Rivers Entering the Arctic Ocean

River	$\delta^{18}O$ (‰)	Discharge (km^3 a^{-1})	Citation ($\delta^{18}O$)	Citation (Discharge)
Yenisey[a]	−18.4	656	*Cooper et al.* [2008]	*Cooper et al.* [2008]
Lena[a]	−20.5	566	*Cooper et al.* [2008]	*Cooper et al.* [2008]
Ob[a]	−14.9	373	*Cooper et al.* [2008]	*Cooper et al.* [2008]
Mackenzie[a]	−19.2	322	*Cooper et al.* [2008]	*Cooper et al.* [2008]
Kolyma[a]	−22.2	114	*Cooper et al.* [2008]	*Cooper et al.* [2008]
Pechora	−14.4	108	*Ekwurzel* [1998]	*Becker* [1995]
Severnaya Dvina	−13.3	99	*Ekwurzel* [1998]	*Becker* [1995]
Indigirka	−23.8	49	*Ekwurzel* [1998]	*Pavlov et al.* [1996]
Yana	−21.1	31	*Ekwurzel* [1998]	*Pavlov et al.* [1996]
Olenek	−20.4	30	*Ekwurzel* [1998]	*Becker* [1995]

[a]These estimates are based on year-round sampling and resolve seasonal variations in $\delta^{18}O$ and discharge.

3.4. Sea Ice Meltwater

[34] There is not enough available data to directly determine the mean salinity of sea ice in the Arctic Ocean by gridding ice core measurements. Instead we use the mean sea ice salinity estimate of 4 determined by *Østlund and Hut* [1984]. Due to a similar lack of $\delta^{18}O$ measurements we assign a value of +0.5 for the $\delta^{18}O$ of sea ice, again following *Østlund and Hut* [1984].

[35] Previous studies [*Østlund and Hut*, 1984; *Bauch et al.*, 1995; *Ekwurzel et al.*, 2001; *Meredith et al.*, 2001; *Dodd et al.*, 2009; *Rabe et al.*, 2009] have estimated specific sea ice $\delta^{18}O$ values at each sampling site based on the surface $\delta^{18}O$ value at each site, plus a constant offset. This approach is valid in studies where sea ice melts and forms in the same place, but much of the sea ice meltwater and brine in Fram Strait forms remotely, so we prefer to use a mean value for the Arctic Ocean.

[36] Due to a paucity of measurements the N:P ratio of sea ice in the Arctic Ocean is unknown. Here we assume that the majority of sea ice in the Arctic Ocean forms from Atlantic-derived, rather than Pacific-derived surface waters. We assign sea ice meltwater a similar N:P ratio to Atlantic seawater.

3.5. Meteoric Water

[37] Pure meteoric water has a salinity of 0. To determine the mean $\delta^{18}O$ of meteoric water in the Arctic Ocean we follow the example of *Østlund and Hut* [1984] and *Ekwurzel et al.* [2001] who use a flow-weighted mean $\delta^{18}O$ value calculated using measurements from the ten largest rivers entering the Arctic Ocean. Here we use more recent observations [*Cooper et al.*, 2008] that resolve seasonal variations in both $\delta^{18}O$ and discharge (Table 3) where possible. We determine a value of −18.4‰, which is comparable with Ekwurzel et al.'s 2001 estimate of −18‰. We neglect direct precipitation into the Arctic Ocean (estimated at 2000 km^3 a^{-1} [*Serreze et al.*, 2006]). The mean $\delta^{18}O$ of direct precipitation is unknown, but it should be similar to the $\delta^{18}O$ of river water entering the Arctic Ocean.

[38] We assume that meteoric water does not experience significant nitrification or de-nitrification en-route to the Arctic Ocean and assign the Atlantic seawater N:P ratio to Meteoric water. The real N:P ratio of meteoric water is likely to be different from that of Atlantic water. However, setting a common value for the N:P ratio of Atlantic water, meteoric water and sea ice meltwater is advantageous as it prevents relatively large uncertainties in the N:P ratio of Atlantic water from affecting the fractions of meteoric water and sea ice meltwater determined.

3.6. Error Analysis

[39] The inaccurate specification of end-member property values is by far the largest source of error in our calculations, but it is difficult to quantify the uncertainty in these values. Here we present a sensitivity test in which the values for each end-member property are varied from the lowest to the highest values that we think are feasible, based on the literature. Figure 6 shows how these variations affect the derived freshwater composition for a typical sample. From this sensitivity test we estimate the following uncertainties in each fraction: meteoric water: 1%, sea ice meltwater: 1%, Pacific seawater: 10%, Atlantic Seawater: 10%. Our estimates are similar to those of *Bauch et al.* [2011], *Yamamoto-Kawai et al.* [2008], *Jones et al.* [2008a], *Taylor et al.* [2003] and *Bauch et al.* [1995] who use similar mass balance equations. Our first priority is to study how the relative composition of the freshwater outflow at Fram Strait has changed through time, rather than to determine the absolute composition at any one time. As our end-members do not vary in time we expect that the relative accuracy of freshwater fractions determined in different years is rather better than the absolute accuracy.

4. Spatial Distribution of Freshwater Components at Fram Strait

4.1. Spatial Distribution of Sea Ice Meltwater

[40] Figure 7 shows the net fraction of sea ice meltwater along each section. Net fractions of sea ice meltwater are generally negative in the EGC and the Arctic Ocean outflow over the East Greenland Shelf, due to the net formation of sea ice in the Arctic Ocean. In western Fram Strait negative sea ice fractions extend from the surface to a depth of 250–300 dbar in the EGC and over the East Greenland Shelf in the region occupied by Polar Surface Water (PSW) as defined by *Rudels et al.* [2002].

[41] At the surface, sea ice melts into PSW, increasing the net fraction of sea ice meltwater in the upper 0 to 25 dbar. However, the net fraction of sea ice meltwater generally remains negative. Due to the addition of sea ice meltwater at the surface, net sea ice meltwater fraction minima are typically found at depths of 25 to 50 dbar. When sea ice melts to the east of the EGC, where underlying net sea ice meltwater fractions are close to zero, patches of positive sea ice meltwater may be formed. The scale used in Figure 8 revels the

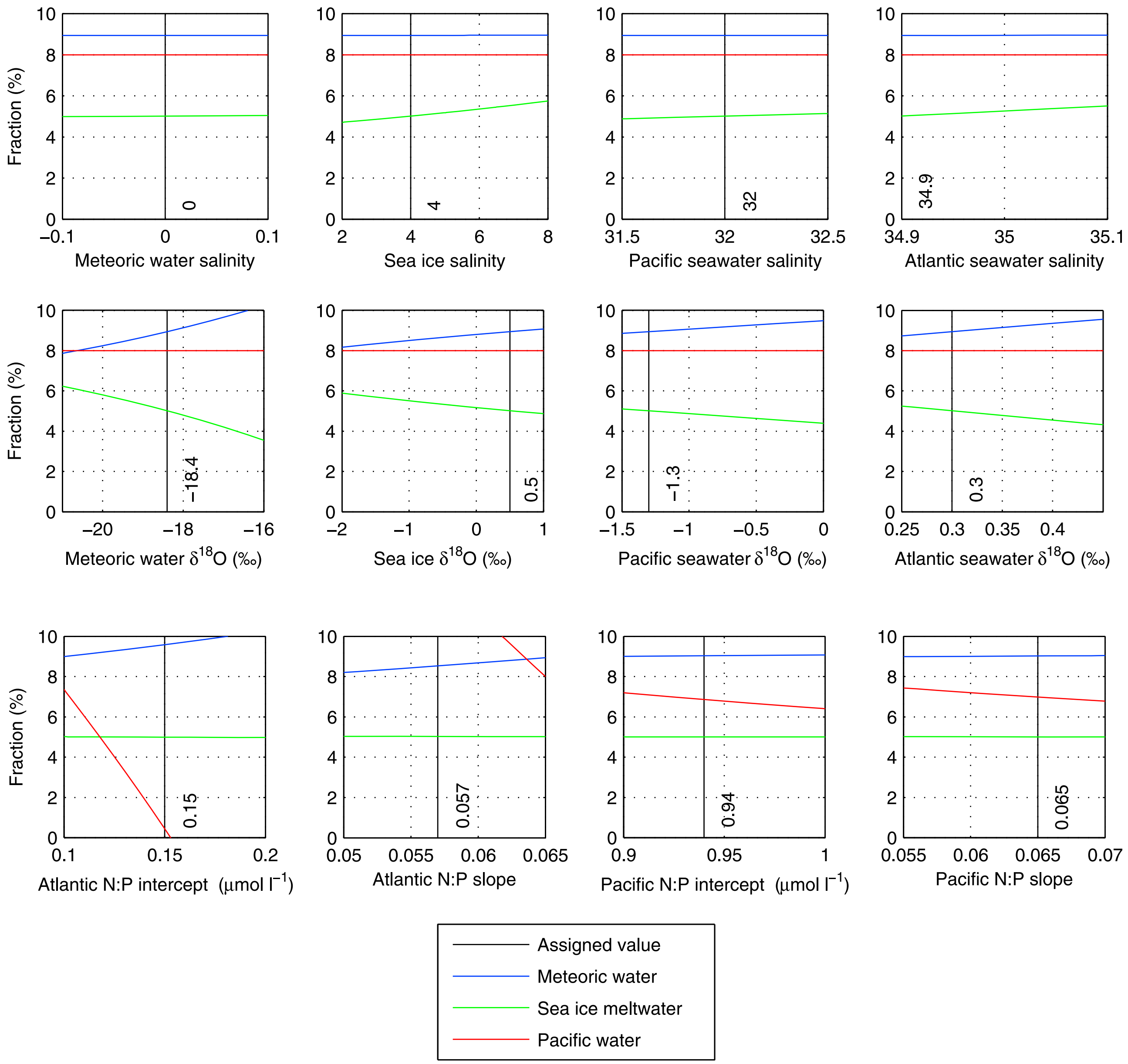

Figure 6. Sensitivity test results showing how uncertainties in each end-member property affect the derived freshwater composition for a sample of idealized polar surface water consisting of: 78% Atlantic seawater, 8% Pacific seawater, +5% sea ice meltwater and 9% meteoric water. Such a sample has the following properties: Salinity = 29.948, $\delta^{18}O = -1.49$‰, N = 5.00 μmoll^{-1}, P = 0.51 μmoll^{-1}. In this sensitivity analysis each property of each end-member is varied between the minimum and maximum feasible value.

distribution of positive net sea ice meltwater in the upper 50 dbar more clearly than Figure 7.

[42] In recent September sections (September 2009–September 2011) broad patches of positive sea ice meltwater are observed between 0 and 5 W, close to the core of the EGC. A small patch of positive sea ice meltwater was also observed in this region in September 1997. The patches are always located just to the east of the main freshwater outflow as defined by sub-surface net sea ice meltwater fractions.

[43] In September 2008 a very broad and deep patch of positive sea ice meltwater seems to have existed between 0 and 5 E, with surface fractions exceeding 8%. It is possible that this patch extended to 4 W much like the meltwater patches observed from September 2009 to September 2011. The western boundary of the patch cannot be determined in the September 2008 section due to a lack of sampling between 0 and 5 W.

[44] The presence of sea ice meltwater in eastern Fram Strait is an important observation regarding the fate of freshwater exported from the Arctic Ocean, because it suggests that sea ice has a greater capacity to escape from the EGC than liquid freshwater, which is trapped by the strong density gradient between the EGC and adjacent gyres.

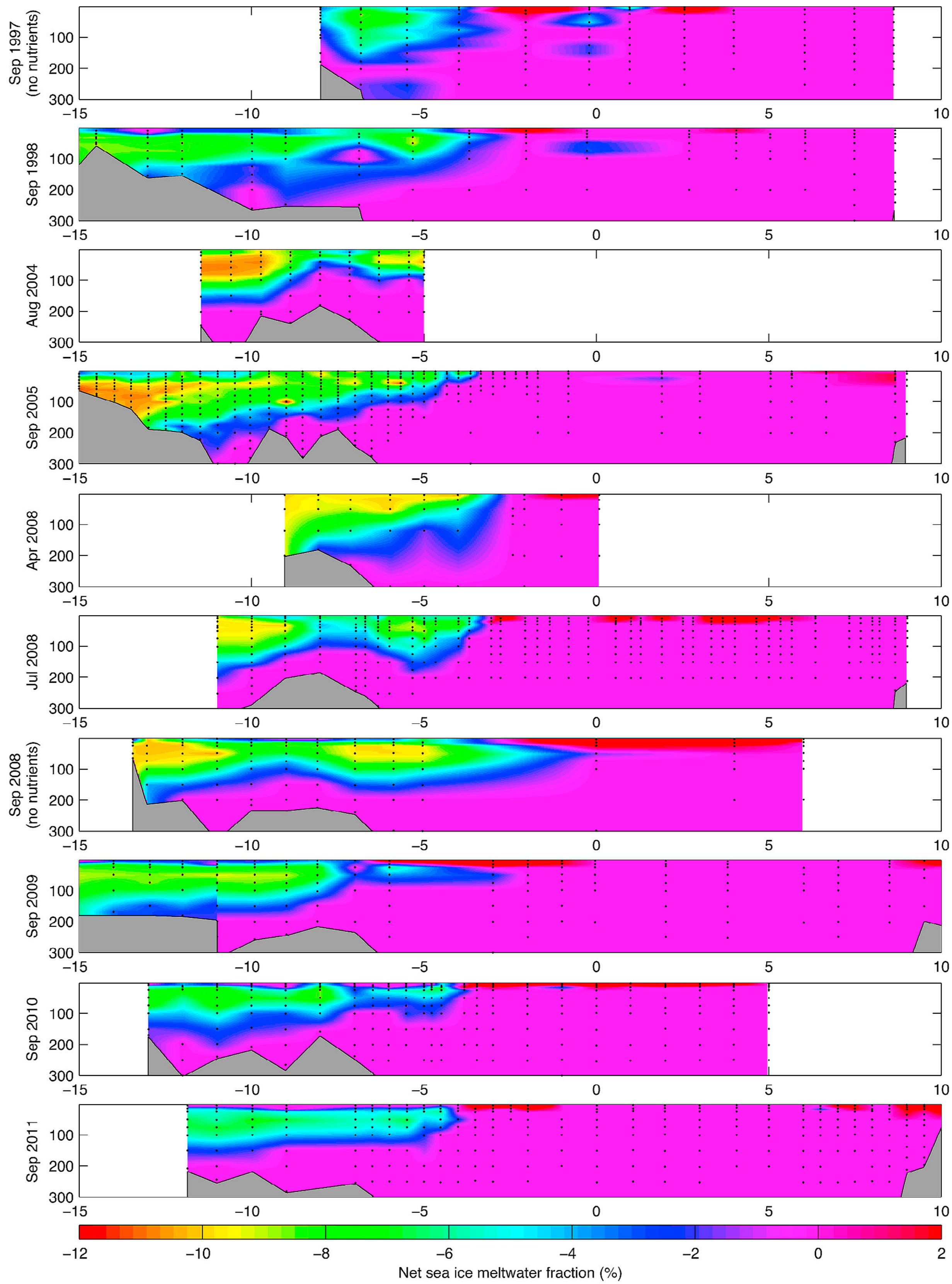

Figure 7. Sections of net sea ice meltwater fractions across Fram Strait. Black dots indicate sampling locations. $\delta^{18}O$ samples were not collected between 5 W and 10 W in September 2005. These $\delta^{18}O$ values were reconstructed from salinity measurements using the $\delta^{18}O$ salinity relationship determined between 5 W and 10 W in August 2004.

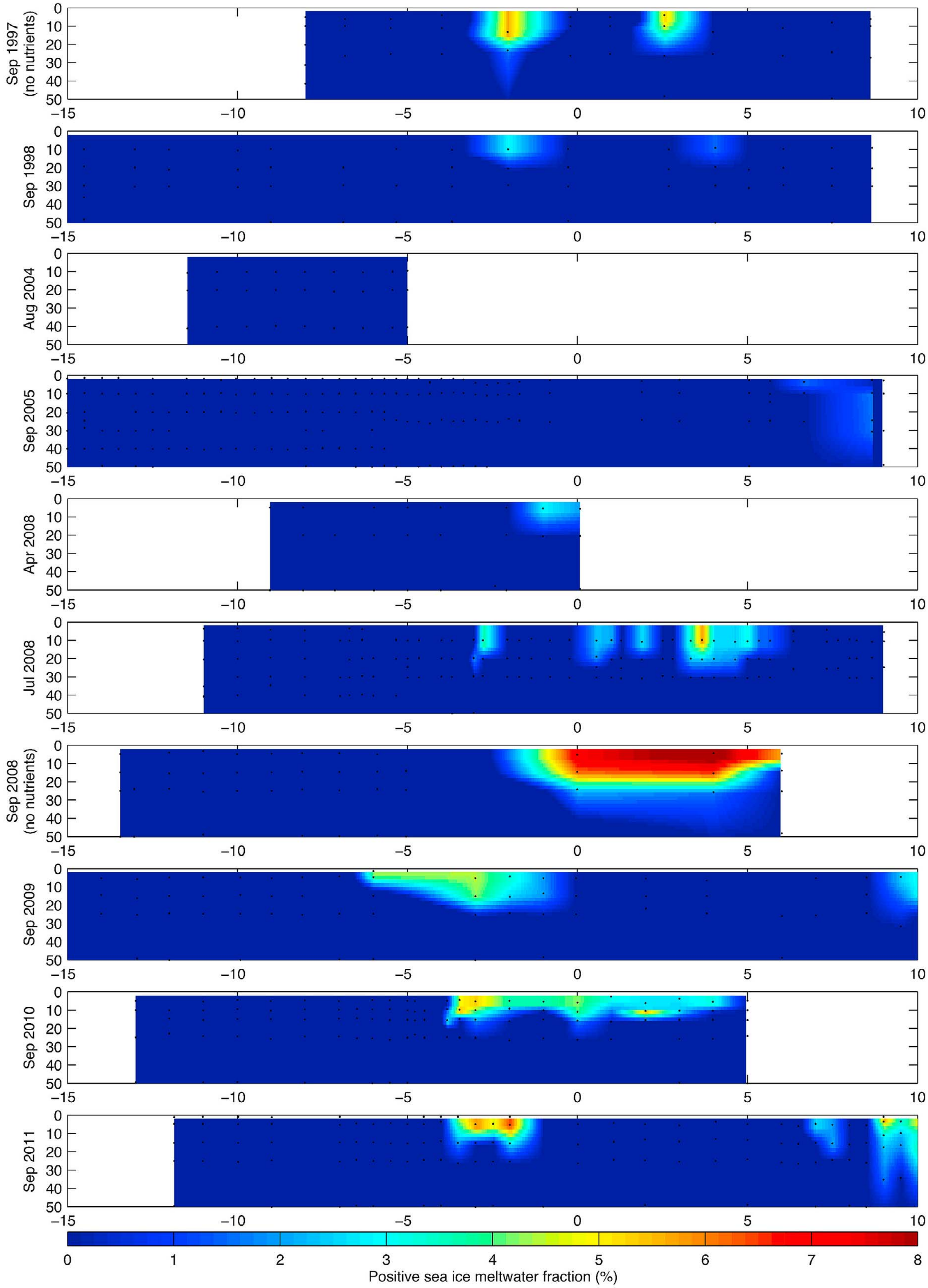

Figure 8. Sections of positive sea ice meltwater fractions across Fram Strait. Black dots indicate sampling locations. $\delta^{18}O$ samples were not collected between 5 W and 10 W in September 2005. These $\delta^{18}O$ values were reconstructed from salinity measurements using the $\delta^{18}O$ salinity relationship determined between 5 W and 10 W in August 2004.

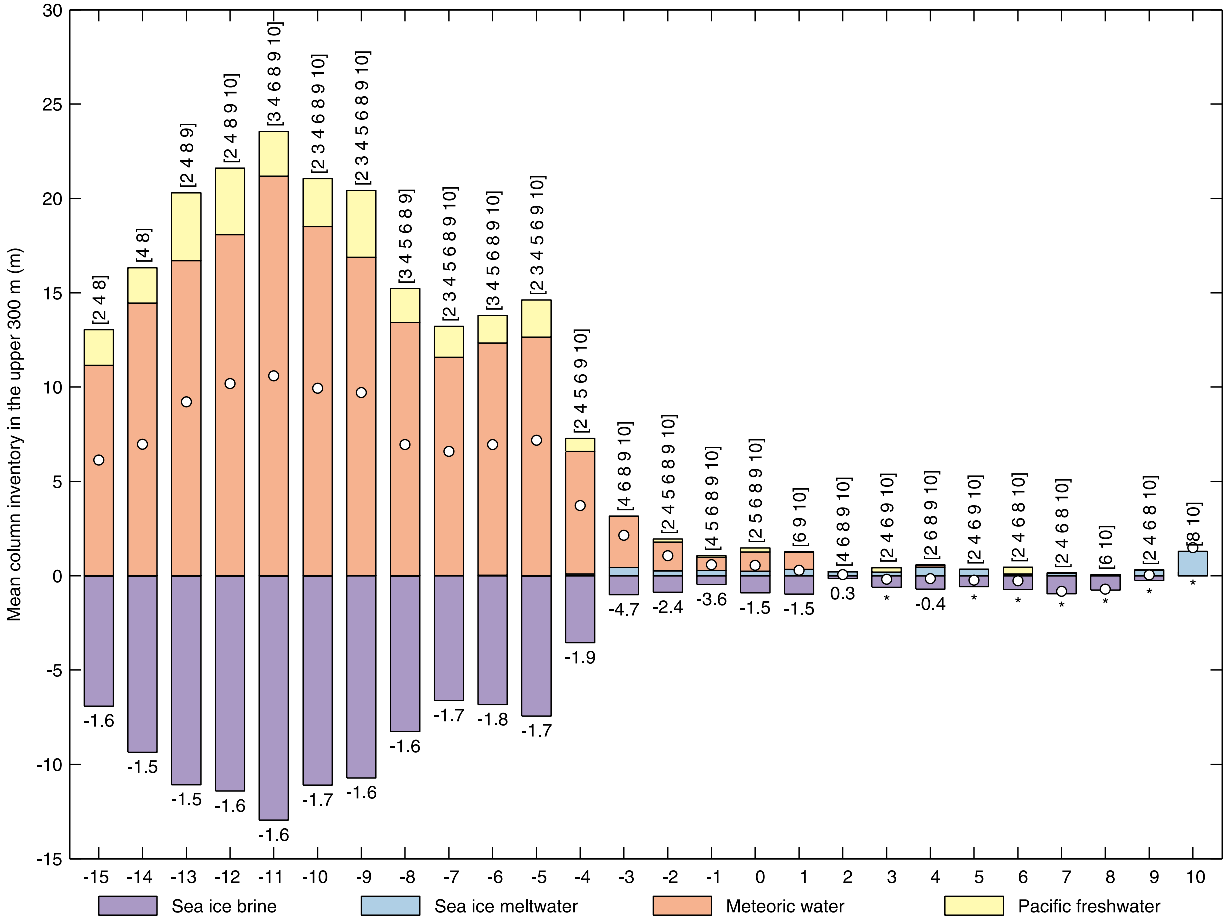

Figure 9. Mean inventories of sea ice brine, sea ice meltwater, meteoric water and Pacific freshwater at Fram Strait above 300 meters (in meters). Mean inventories were calculated after binning profiles from all cruises into 1 degree wide bins. Not all cruises are included in all bins due to the differing extent of sections. Numbers in brackets above each bar indicate the cruises that were included: cf. Table 1. The position of the white dots indicates the net freshwater inventory. The ratio of net sea ice meltwater to meteoric water inventories is printed below each bar. Where the meteoric water inventory was ≤0 an asterisk is printed in place of a ratio. Due to our choice of reference salinity (34.9), small negative (>−0.5 m) meteoric water inventories arise within the saline (≃35.2) West Spitsbergen Current in western Fram Strait. For clarity, negative inventories are not plotted.

[45] Figure 9 shows the mean column inventories of sea ice meltwater, sea ice brine (negative net sea ice meltwater), meteoric water and Pacific freshwater across Fram Strait in 1-degree wide bins. Because some sections are longer than others the number of profiles averaged in each bin varies. Numbers above each bar indicate which sections are included in each bin (cf. Table 1). Note that profiles from September 1997 and September 2008 are never included as nutrient samples (required to separately identify the Pacific freshwater fraction) were not collected along these sections. Figure 9 highlights the location of sea ice brine adjacent to the EGC east of 5 W. The figure also shows that the column inventories of positive sea ice meltwater in Fram Strait are small compared to the inventories of sea ice brine (negative net sea ice meltwater).

[46] As demonstrated in Figure 9, it is possible to divide inventories of net sea ice meltwater into positive sea ice meltwater (positive sea ice meltwater fractions) and brine from sea ice formation (negative sea ice meltwater fractions) by integrating the fractions of negative and positive sea ice meltwater separately. However, separately integrated inventories of sea ice meltwater and brine need to be interpreted carefully due to the different effects of vertical mixing in each year. In years with strong vertical mixing the thin surface layer of meltwater may be mixed into a much thicker layer of underlying brine. In this situation the surface meltwater would be completely obscured while the fraction of underlying brine would be only slightly reduced. If sea ice meltwater and sea ice brine are mixed it is not possible to distinguish between the two without an additional tracer. Separately integrated sea ice meltwater and brine inventories should probably not be compared between sections from different years. Rather, the net sea ice meltwater inventory should be compared instead.

[47] In both Eastern and Western Fram Strait fractions of net sea ice meltwater are highest (least negative) at the surface (Figure 7). This is unsurprising as sea ice melts and

releases freshwater at the surface. But where does this melting occur geographically?

[48] The thin surface layer is well stratified, with a strong salinity gradient. This stratification may mean the layer is resistant to vertical mixing. If the layer does resist vertical mixing, it might contain meltwater from sea ice melting far upstream of Fram Strait. On the other hand, positive fractions of sea ice meltwater found outside of the EGC suggest that at least some sea ice probably melts in Fram Strait.

[49] The surface fraction of sea ice meltwater in Fram Strait seems to respond quickly to seasonal variations in the local sea ice extent (cf. April 2008, July 2008 and September 2008 sections in Figures 7 and 8). If significant meltwater input occurred far upstream of Fram Strait, we would expect surface sea ice meltwater maxima to lag the September minimum sea ice extent in Fram Strait. However, without tracer measurements between October and March we cannot properly assess the lag between the minimum sea ice extent and maximum surface sea ice meltwater fractions.

[50] *Wadhams et al.* [1992] used an upward looking sonar mounted on a submarine to construct histograms showing the thickness distribution of sea ice in the EGC at different latitudes. *Wadhams et al.* [1992] found that the sea ice thickness distribution changed dramatically at Fram Strait. In their 1982 data set much less multi-year and deformed sea ice (between 4–11 meters thick) was found to the south of Fram Strait, while the amount of undeformed first year sea ice (around 2 meters thick) was similar north and south of Fram Strait. This suggests that thick sea ice is preferentially removed at Fram Strait. The preferential removal of thick ice at Fram Strait supports the hypothesis that the surface meltwater layer we observe in western Fram Strait forms locally when thicker sea ice drifting out of the Arctic Ocean encounters warm re-circulating Atlantic water. Thicker sea ice penetrates deeper into the ocean than thinner ice and is more susceptible to melting from oceanic heat input than thinner ice.

4.2. Spatial Distribution of Meteoric Water

[51] Figure 10 shows the fraction of Meteoric water in Fram Strait along each section. Below the surface 25 dbar (away from the direct influence of sea ice meltwater input) the distribution of meteoric water correlates well with the distribution of negative net sea ice meltwater (cf. Figures 7 and 10). Most of our sections across Fram Strait show two separate, surface-intensified meteoric water maxima: one in the EGC and one over the East Greenland Shelf (Figure 10). Over the East Greenland Shelf meteoric water generally penetrates to the sea bed at 300 dbar, but little meteoric water is found below 180 dbar in the EGC. The lesser penetration of meteoric water in the EGC is presumably due to the presence of recirculating Atlantic water (defined by *Rudels et al.* [2002]) below about 180 dbar in the EGC, which is absent over the shelf. In some sections (e.g., August 2004 and July 2008) very well defined, separate meteoric water fraction maxima occur over the East Greenland Shelf and in the EGC. In other years (e.g., September 2005, September 2009, September 2010, September 2011) the EGC maximum is much reduced.

[52] Our longest sections, which extend almost to the Greenlandic coast at 17 W, show that about two-thirds of the total meteoric water and brine inventories in Fram Strait reside over the East Greenland Shelf west of 8 W (Figure 11, middle row). The circulation over the East Greenland Shelf beyond 8 W is not as well known as the circulation further east, where moored current meters have provided a long time series of measurements and the fate of this shelf water is not certain. Cumulative inventories within Figure 11 are reported in units of km^2. These are calculated by first calculating the column inventory at each station and then integrating horizontally along sections.

4.3. Spatial Distribution of Pacific Freshwater

[53] Figure 12 shows the fraction of Pacific freshwater in Fram Strait along each section. Significant Pacific freshwater fractions are found in the EGC and over the East Greenland Shelf in Fram Strait. In September 1998 and July 2008 separate, well defined maxima occurred over the shelf and in the EGC. Maximum Pacific freshwater fractions are found at the western end of sections over the East Greenland Shelf, except in September 2011, when the maximum Pacific freshwater maximum was in the ECG.

[54] The Bering Strait is only about 80 m deep, so it is unsurprising that the majority of Pacific freshwater is found in the top 80 dbar at Fram Strait. In sections with low surface fractions of Pacific freshwater (August 2004, September 2005, September 2009, September 2010), significant fractions of Pacific freshwater are only found between the surface and 100 dbar. However, in sections with higher Pacific freshwater fractions at the surface (September 1998, April 2008 and September 2011), Pacific freshwater seems to penetrate significantly deeper reaching about 150 dbar.

[55] Some low Pacific freshwater fractions appear at around 6 E in our July 2008 section. These fractions are confined to one CTD station and occur at a Pacific seawater fraction level that is close to our detection limit if we assume a 10% precision when differentiating between Pacific seawater and Atlantic seawater (section 3.6). We do not think these points indicate the presence of Pacific freshwater in eastern Fram Strait.

4.4. Spatial Distribution Summary

[56] The long term mean distribution of freshwater fractions in Fram Strait is summarized in Figure 9. Figure 9 highlights the existence of two freshwater maxima: one over the East Greenland Shelf and one in the core of the EGC (at 5 W) over the shelf break. The ratio of MW:SIM inventories at each degree longitude is printed on Figure 9. In general the freshwater composition is similar in the core of the EGC and over the East Greenland Shelf, but from 3 W to 2 E small inventories of positive sea ice meltwater are typical. East of 2 E, there are no significant freshwater inventories and the composition appears much more variable. However, the fractional inventories found east of 2 W are typically only a few meters and are close to the limit of detection estimated in section 3.6.

5. Temporal Changes in the Composition of Freshwater at Fram Strait

5.1. Mean Composition Between 1998 and 2011

[57] The EGC follows the shelf break along the coast of East Greenland [*Rudels et al.*, 2002], which occurs at about 5 W in our sections. In this section we discuss the

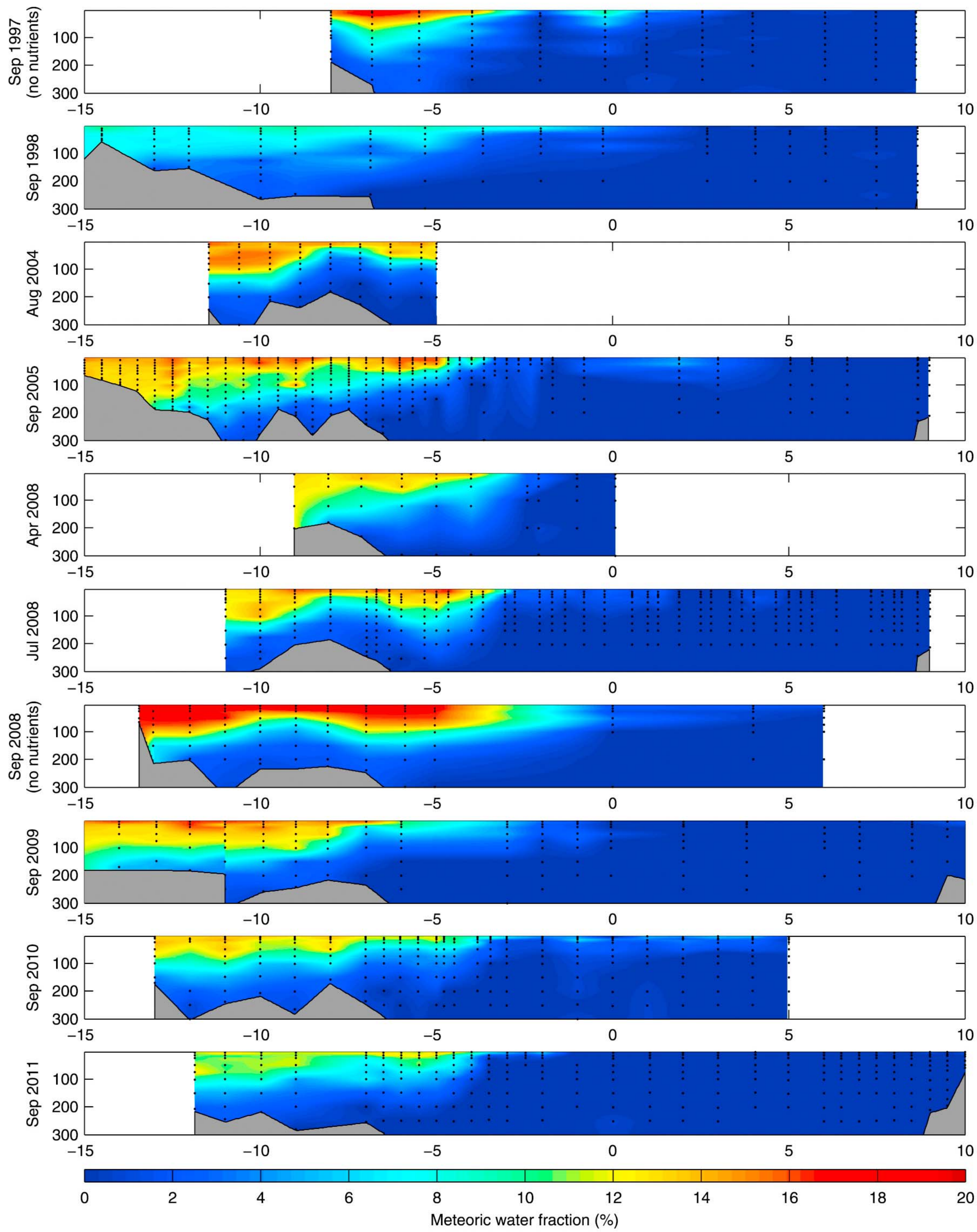

Figure 10. Sections of meteoric water fractions across Fram Strait. Black dots indicate sampling locations. $\delta^{18}O$ samples were not collected between 5 W and 10 W in September 2005. These $\delta^{18}O$ values were reconstructed from salinity measurements using the $\delta^{18}O$ salinity relationship determined between 5 W and 10 W in August 2004. In September 1997 and September 2008 the meteoric water fraction includes any Pacific water that was present at Fram Strait, which was not separately determined along these sections.

composition of the freshwater inventory between 0 and 10 W. As the EGC is a boundary current constrained by the bathymetry it should always be contained within this region. Studying a consistent region allows us to compare the freshwater composition of the EGC at different times without having to account for the length of each section. Figure 13 summarizes the inventory of each freshwater component between 0 and 10 W along each section.

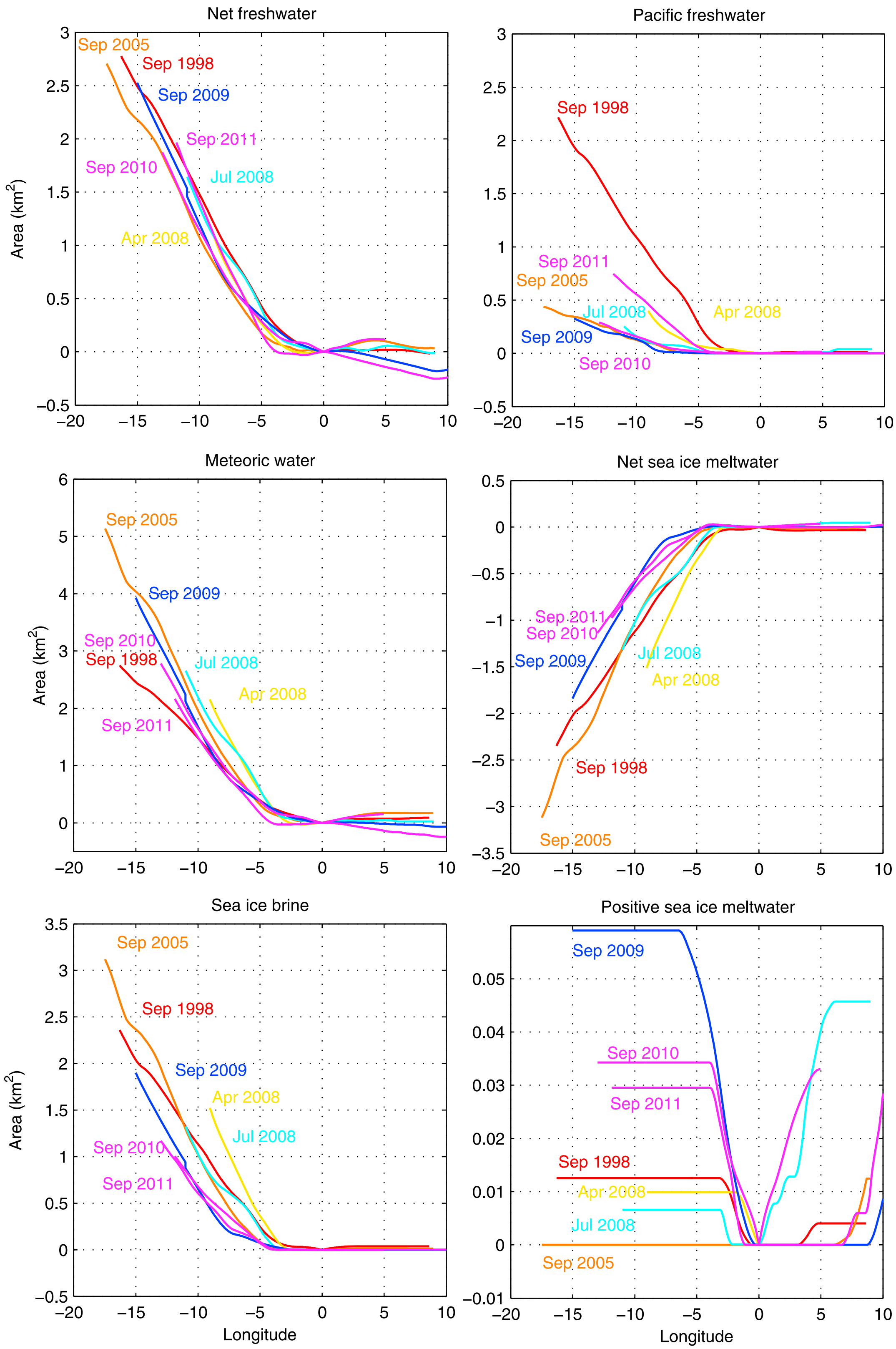

Figure 11. Plots showing cumulative inventories of net freshwater, Pacific freshwater, meteoric water, net sea ice meltwater, brine from sea ice formation and positive sea ice meltwater across Fram Strait for each year data were collected. Cumulative inventories were calculated from the Greenwich meridian (integrating westwards in the western hemisphere and eastwards in the eastern hemisphere). Cumulative inventories are not plotted for September 1997 or September 2008 due to a lack of N and P measurements or for August 2005 when the section was very short.

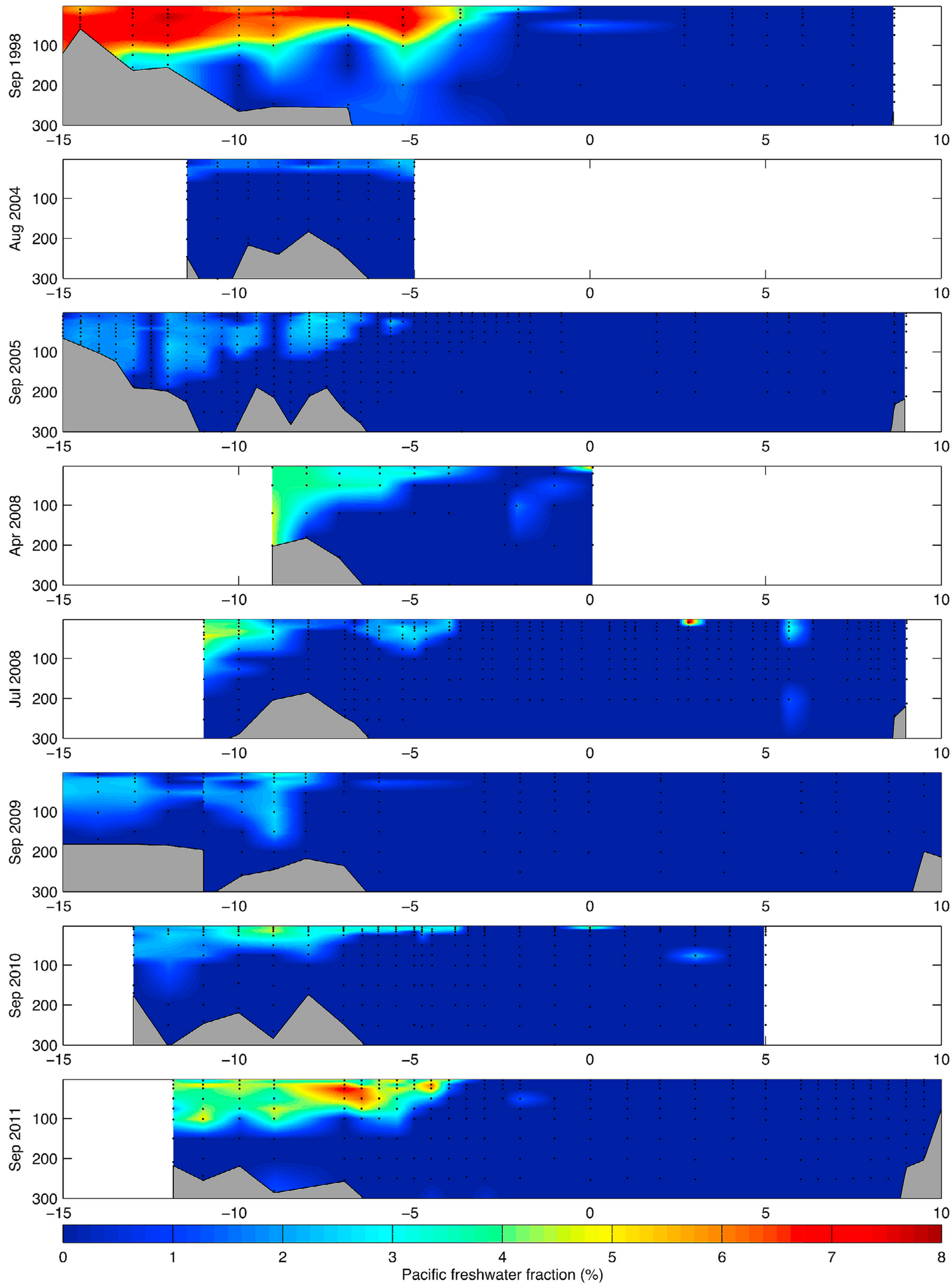

Figure 12. Sections of Pacific freshwater fractions across Fram Strait. Black dots indicate sampling locations. Sections are not plotted for September 1997 or September 2008 because dissolved NO_3^+ and P concentration measurements required to determine the concentration of Pacific freshwater were not collected along these sections.

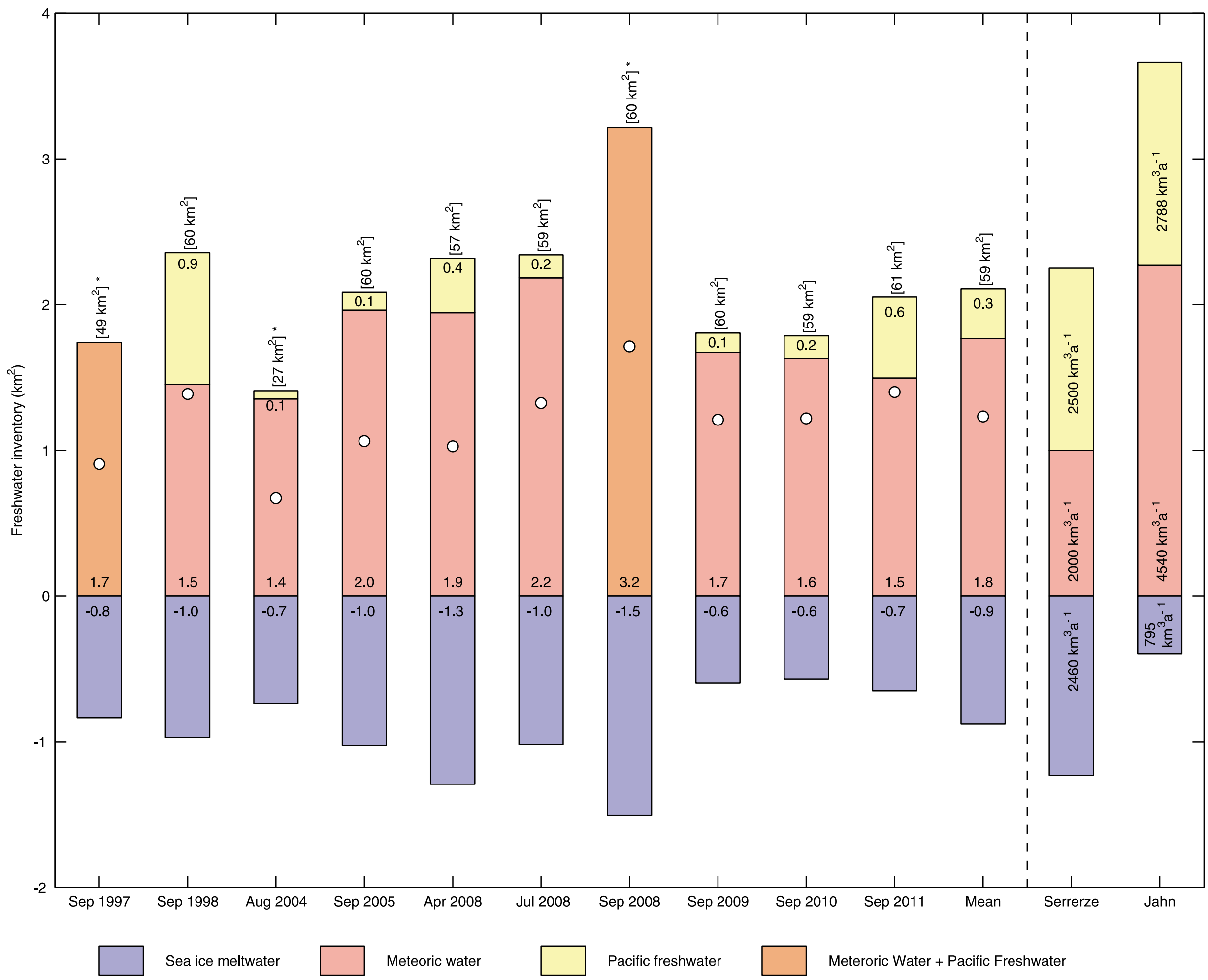

Figure 13. Inventories of net sea ice meltwater, meteoric water and Pacific freshwater at Fram Strait above 300 dbar between 10 W and the Greenwich meridian. Where the Pacific freshwater and meteoric water could not be separated due to a lack of nutrient measurements the combined inventory is plotted in orange. The total water area of each section is shown in brackets above each bar. Numbers within each bar segment indicate the inventory of that freshwater component in km^2. Bars marked with an asterisk were excluded when calculating the mean bar. The position of the white dots indicates the net freshwater inventory in km^2. Bars on the right show the volume transport of each freshwater fraction through Fram Strait listed in the studies of *Serreze et al.* [2006] and *Jahn et al.* [2010].

[58] Considering only sections that completely span the study region and that feature concurrent δ^{18}O and N:P ratio measurements (September 1998, September 2005, July 2008, September 2009, September 2010 and September 2011) we determine the following mean composition for freshwater in the EGC in late summer: meteoric water: 1.8 km^2, net sea ice meltwater: -0.9 km^2 (-0.9 km^2 brine + 0.03 km^2 meltwater) and Pacific freshwater: 0.3 km^2 (Figure 13). We exclude inventories from the September 1997 and April 2008 sections, which lack nutrient measurements and the inventory from the August 2004 section, which spans only half the study region. Sections excluded from the mean are marked with asterisks on Figure 13.

[59] The mean freshwater composition determined from our selected sections includes a smaller proportion Pacific freshwater than might be expected from the freshwater budget of *Serreze et al.* [2006]. *Serreze et al.* [2006] estimate the Pacific water input into Arctic Ocean using measurements from the Bering Strait collected by *Woodgate and Aagard* [2005] between 1990 and 2004. *Falck et al.* [2008] show that the fraction of Pacific water at Fram Strait is highly variable and that high fractions of Pacific water (comparable with levels in our 1998 section) prevailed from 1990 to 1993 and from 1997 to 1999. It is possible that we missed some high fractions of Pacific water at Fram Strait between 2005 and 2008 (section 4.3) and that our mean value is low as a result. However, it is also possible that the mean fraction of Pacific water at Fram Strait was indeed lower during our study than during the previous decade.

[60] Within our study region the meteoric water inventory of selected sections varied by -10% and +31% relative to the mean. The net sea ice meltwater inventory of selected sections was somewhat more variable, varying by -44% and +22% relative to the mean. The mean ratio of meteoric water to net sea ice meltwater (MW:SIM) in our sections

was −2:1. Although the ratio varied in time (discussed in sections 5.3 and 5.4), the long term mean ratio did not vary much between the EGC and the East Greenland Shelf (Figure 9). Therefore, the ratio determined between 0 and 10 W should be representative of the Fram Strait freshwater outflow in general.

[61] *Bauch et al.* [1995] and *Meredith et al.* [2001] both determine MW:SIM ratio values of about −2:1 at Fram Strait. Our September 1998 section uses the same salinity and δ^{18}O measurements as *Meredith et al.* [2001]. However, with the benefit of concurrent N:P ratio measurements we separately identify a significant Pacific freshwater water inventory (Figure 13, 2nd bar from left).

[62] In *Serreze et al.*'s [2006] freshwater budget the meteoric water transport through Fram Strait is only about −0.8 times the net sea ice transport. *Serreze et al.* [2006] estimate the meteoric water input into Arctic Ocean using measurements and re-analysis products for the years 1979 to 2001 and estimate the sea ice transport using moored sonar data from 1990 to 1996 [*Vinje et al.*, 1998]. The mean freshwater composition determined from our (1998 to 2011) observations reveals a larger proportion meteoric water at Fram Strait than expected from the freshwater budget of *Serreze et al.* [2006].

[63] *Serreze et al.* [2006] consider the complete Fram Strait outflow from the Arctic Ocean, while we only consider the outflow between 0 and 10 W. Extending our integration region to the east would not change the mean integrated freshwater composition significantly, because there are no significant inventories of freshwater or brine east of the Greenwich meridian (Figure 9). Extending our integration area to the west would include large inventories of freshwater and brine residing on the East Greenland Shelf. However, the ratio of sea ice meltwater : meteoric water : Pacific freshwater over the East Greenland Shelf is similar to that within our integration region (Figure 9).

5.2. Seasonal and Interannual Variability

[64] Figure 14 shows vertical cumulative inventory profiles for each freshwater fraction in our (0 to 10 W) study region. Fractions that were not significantly different from zero were set to zero before the integration exercise. Due to the imperfect specification of end-members small (<0.1%) spurious fractions are found over large areas of deep water. These spurious fractions add up to significant inventories if they are not eliminated.

[65] We also adjust the vertical cumulative inventories for September 1998 and April 2008. Very few samples were collected from depths between 150 and 300 dbar in these sections and this lack of sampling causes spuriously large inventories to be calculated in this depth range due to non-linear gradients. So that profiles from September 1998 and April 2008 can be directly compared with other years we have applied an offset so that the September 1998 and April 2008 inventories equal the mean inventory of all other sections at 150 dbar. Above 150 dbar the sampling density was similar along all sections. The un-adjusted cumulative inventories for September 1998 and April 2008 are plotted as dashed black lines on Figure 14. Note that the inventories presented in Figure 13 were also adjusted in the same way as those presented in Figure 14.

[66] The shape of net sea ice meltwater inventory profiles (Figure 14, middle row, right panel) seems to vary seasonally due to the advance and retreat of sea ice. The minimum sea ice extent in Fram Strait occurs in September and recent (2009–2011) September cumulative inventory profiles recurve strongly in the top 25 m, suggesting that sea ice meltwater has been added at the surface. The inventory profile from April 2008 (collected soon after the maximum sea ice extent, when freezing conditions prevail) does not show this recurve at all. Cumulative inventory profiles collected earlier in the summer in July 2008 and September 2005 show very slight recurve, note that data-gaps in the September 2005 section were filled using data collected from *July* 2004 as discussed in section 2. The cumulative inventory profile from September 1998 shows some recurve, but not as much as recent (2009–2011) September sections.

[67] The inventory and the shape of the inventory profiles is strikingly similar in recent September sections and markedly different from previous profiles. It is unclear if this is due to seasonal variability or if it is indicative of long term change. To induce the recurve seen in recent September profiles in a profile with a shape similar to the September 1998 or September 2005 profiles would require the addition of about 0.1–0.2 km^2 of sea ice meltwater (see dotted extensions to September 2009–2011 profiles on Figure 14, middle row, right panel). This is about 10–20% of the September 1998 or September 2005 net sea ice meltwater inventories.

[68] The recent recurved profile shape may indicate that (very approximately) 10–20% of the net volume of sea ice formed in the Arctic now melts back into the surface north of Fram Strait in September where as before 2009 almost none melted back.

[69] Comparing the net sea ice meltwater inventories in April and July 2008 shows a change of 0.3 km^2 (a 30% increase). This change seems to be a combination of seasonal and interannual variability. The April 2008 meteoric water inventory is also 0.3 km^2 more than the July 2008 inventory (an increase of about 16%) but there is no reason to expect seasonal variability in the meteoric water inventory at Fram Strait. If we decrease the sea ice meltwater inventory in July 2008 by 16%, to account for the interannual part of the variability suggested by the change in meteoric water inventory, we get a 'corrected' net sea ice meltwater inventory of −1.2 km^2. Which is about 0.1 km^2 more than the April 2008 inventory. It seems reasonable that 0.1 km^2 of sea ice meltwater was added to the water column between April and July 2008 as a result of seasonal sea ice melting. 0.1 km^2 is equivalent to a mean sea ice thickness reduction of 0.5 m along the 212 km long study region between 0 to 10 W.

[70] Cumulative inventory profiles of meteoric water (Figure 14, middle row, left panel) have a highly consistent shape compared with the net sea ice meltwater profiles. The consistent shape suggests that variations in the meteoric water inventory generally arise from whole water column changes in the meteoric water fraction, rather than from variations in a particular depth range.

[71] Very high Pacific freshwater fractions were observed at Fram Strait in September 1998 (Figures 13 and 14, top rows, right panels). However, while the September 1998 section is exceptional among the sections presented in this paper, it is not unusual in a broader context. The fraction of

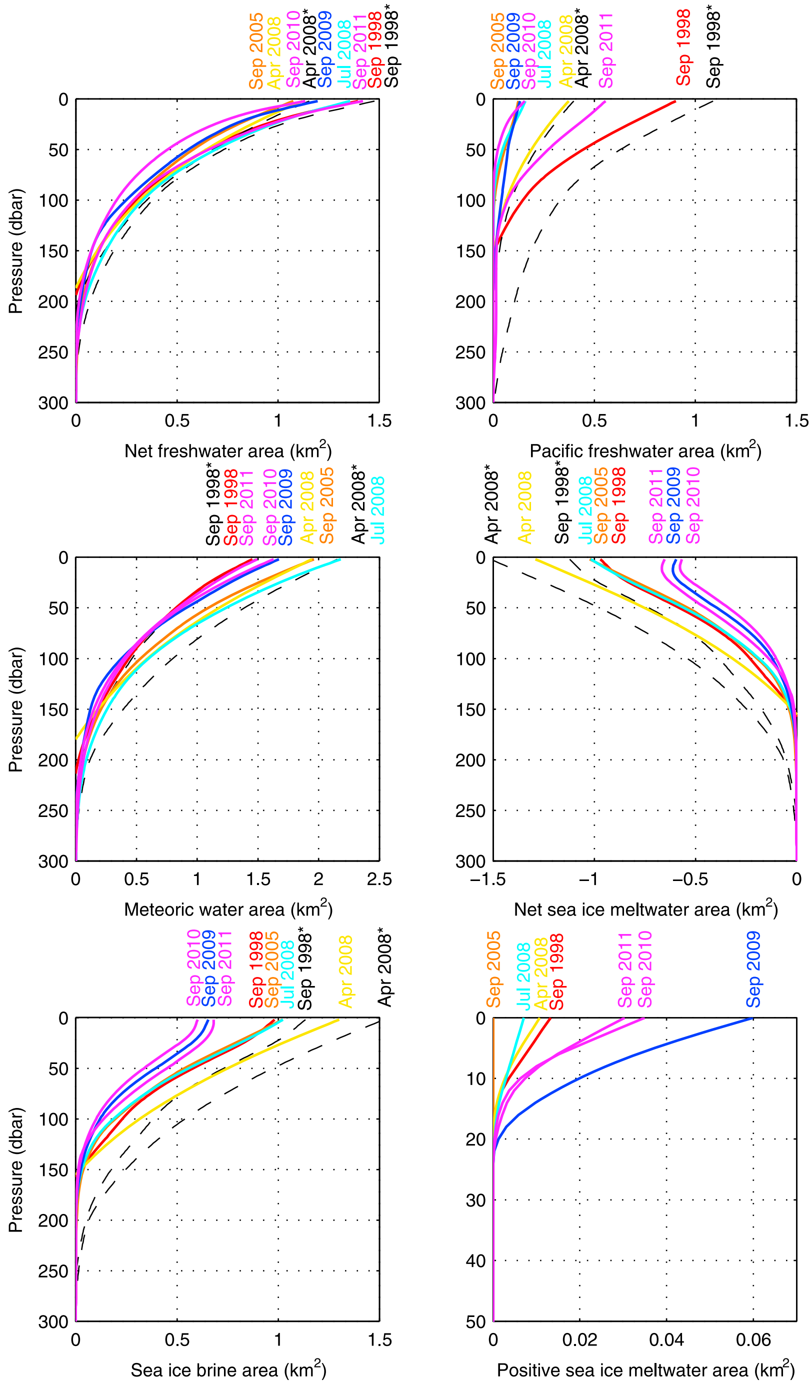

Figure 14. Plots showing cumulative inventory profiles for net freshwater, Pacific freshwater, meteoric water, net sea ice meltwater, brine from sea ice formation and positive sea ice meltwater across Fram Strait for each year data were collected. The integration was performed between 10 W and the Greenwich meridian -or to the end of the section where sections did not span this region. Cumulative inventory profiles were calculated from the bottom of the water column to the surface. Inventories are not plotted for September 1997 or September 2008 due to a lack of N and P measurements or for August 2005 when the section was very short.

Pacific water has been monitored at Fram Strait since 1984 [*Falck et al.*, 2005] and similar fractions occurred in June 1990, June 1991 and May 1993. Fractions comparable with the majority of the sections presented here also occurred in July 1984, June 1988 and September 1995.

[72] *Falck et al.* [2005] reported that Pacific water had 'all but disappeared' from Fram Strait based on their analysis of a number sections completed between July 1984 and August 2004. Here we observe the return of significant fractions in April 2008 and September 2011. As we do not have any

measurements between September 2005 and April 2008 we cannot be sure how long the fractions observed in April 2008 prevailed, but they were no longer present in July 2008. Previous sections [*Falck et al.*, 2005] showed high fractions of Pacific water to persist for a few years (e.g., 1990–1993 and 1997–1999), these were separated by periods of low fractions lasting a similar length of time (e.g., 1994–1996).

[73] In September 1998 Pacific freshwater made up 65% of the net freshwater inventory in Fram Strait. But in years with lower fractions (e.g., September 2010) Pacific freshwater contributed only about 15%. Variations in the fraction of Pacific water at Fram Strait therefore contribute significantly to the variability of the net freshwater inventory.

5.3. Gradual Changes Between 1998 and 2008

[74] In general, sea ice meltwater fractions tend to be anticorrelated with meteoric water fractions (Figure 13). Together with the observation that meteoric water and sea ice brine are found in the same locations, the co-variance of sea ice brine and meteoric water fractions suggests that meteoric water and brine are delivered to Fram Strait together.

[75] Much of the meteoric water and brine found at Fram Strait probably originates from the shelf seas of the Eastern Arctic, where large volumes of river water discharged by the Ob, Kahtanga, Olenek, Lena, Yana, Indigirka and Kolyma rivers enter the central Arctic Ocean. In the same region, large polynyas facilitate rapid sea ice formation. Short term variations in the fraction of sea ice meltwater (below 25 dbar) and meteoric water at Fram Strait may be determined by the intermittent release of water from the shelf seas of the eastern Arctic.

[76] *Bauch et al.* [2011] conducted a wide synoptic survey of meteoric water to net sea ice meltwater ratios in the Arctic ocean and observed two distinct regimes. In the southwest Eurasian basin (influenced by the warm Atlantic inflow) large positive fractions of sea ice meltwater are found and river water fractions are typically small. While in the central Arctic Ocean, sea ice meltwater fractions are negative due to sea ice formation and river water fractions are large.

[77] Figure 16 shows meteoric water fractions plotted against sea ice meltwater fractions in our study region between 0 and 10 W in Fram Strait. The majority of subsurface points in Fram Strait lie close to the line formed by a regime modified by open ocean convection as defined by *Bauch et al.* [2011]. Points which lie closer to the relatively fresher shelf and polynya-derived line as defined by *Bauch et al.* [2011] are typically surface (<25 dbar) samples, that correspond to the patches of positive sea ice meltwater discussed in section 4.1.

[78] *Steele et al.* [2004], *Dmitrenko et al.* [2005], *Dmitrenko et al.* [2008] and others suggest release of meteoric water from the East Siberian Shelf may be strongly influenced by the prevailing atmospheric circulation. *Bauch et al.* [2011] and *Guay et al.* [2001] suggest that release of sea ice brine may be affected in a similar way.

[79] If the intermittent release of meteoric water and brine from the Siberian shelves explained all of the variability in sea ice meltwater and meteoric water fractions at Fram Strait, we would expect the ratio of sea ice meltwater to meteoric water at Fram Strait to be fairly constant. However, this is not the case. Figure 15 (top left) shows a steady increase in the meteoric water inventory between 0 and 10 W in Fram Strait with little change in the net sea ice meltwater inventory between 1998 and 2008. The additional meteoric water gradually increased the inventory of meteoric water relative to sea ice meltwater between 1998 and 2008 (Figure 15, bottom left). *Rabe et al.* [2009] also observe a gradual increase in the transport of meteoric water relative to net sea ice meltwater between 1998 and 2005.

[80] High MW:SIM ratios occur in both September 1998 and September 2011. These are the two sections that contained the highest fractions of Pacific freshwater (Figure 15, bottom right). This raises the question of whether we underestimate the y-intercept value for the Pacific seawater N:P relationship and therefore attribute slightly too much freshwater to the Pacific inflow. However, ignoring the data from September 1998 there is still a gradual decrease in the MW:SIM ratio between 2005 and 2008 during which time the Pacific water inventory was negligible.

[81] *Bauch et al.* [2011] note that denitrification over the bottom sediments of the Laptev Sea imparts an artificial Pacific-type signal to sea water in contact with the sediments. However, there is no indication that the extent of this denitrification has changed though time. The magnitude of the artificial signal should remain constant in all our sections.

[82] The gradual changes between 1998 and 2008 may be related to long term changes in the composition of water released from the east Siberian shelves. The gradual changes in the composition of east Siberian shelf water observed at Fram Strait between September 1998 and July 2008 are consistent with larger scale changes observed around the Arctic. For example, the increased proportion of meteoric water is consistent with the increased input of runoff into the Arctic Ocean observed in river gauges around the Arctic Ocean [*Overeem and Syvitski*, 2010]. The increased proportion of net sea ice meltwater is consistent with a reduced volume of Arctic Sea ice in late summer.

[83] The gradual change in the MW:SIM ratio could alternatively be due to increased vertical mixing in the Arctic Ocean associated with a reduced sea ice extent. Mixing sea ice meltwater from the top 25 dbar deeper into the water column might increase the proportion that is exported from the Arctic Ocean rather than being re-incorporated in sea ice during the following ice growth season.

5.4. Rapid Changes Between 2008 and 2011

[84] The 2009, 2010 and 2011 September inventories of sea ice meltwater (calculated between the 0 and 10 degrees west) are the highest (least negative) on record by a large margin (Figure 14, bottom row, left panel and Figure 13). Note that the apparently similar inventories shown for August 2004 on Figure 13 occur because the August 2004 section only spans half of the integration area.

[85] The very high 2009–2011 September net sea ice meltwater inventories result from a combination of low underlying brine fractions and a large input of meltwater at the surface. Net sea ice meltwater inventory profiles (Figure 14, middle row, right panel) recurve steeply at the surface in the 2009–2011 September sections indicating a large surface input of meltwater that has not been observed before as discussed in section 5.2, but Figure 14 (bottom row, left panel) also shows that sea ice brine fractions in the 2009–2011 September sections are low at depths between 25 and 150 dbar.

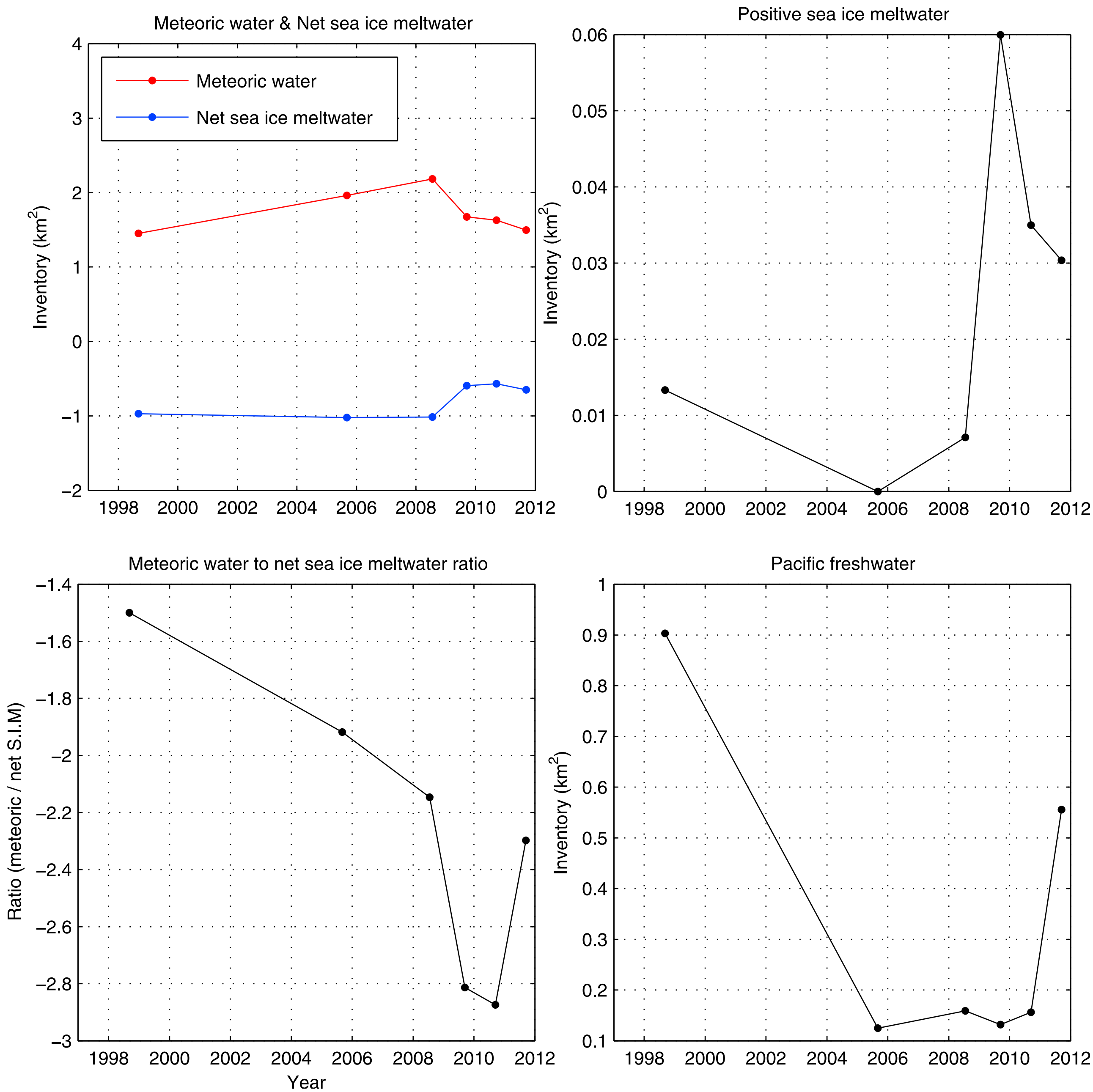

Figure 15. Temporal changes in the inventories of net freshwater meteoric water, net sea ice meltwater and Pacific freshwater and the ratio of meteoric water to net sea ice meltwater at Fram Strait above 300 dbar and between 10 W and the Greenwich meridian. Lines only connect sections where the Pacific freshwater fraction could be separately identified and where the section spanned the complete region between 10 W the Greenwich meridian. Where the section spanned the region but Pacific freshwater was not separately identified, the inventory is plotted as an isolated asterisk.

[86] Between July 2008 and September 2009 the late summer net sea ice meltwater inventory at Fram Strait increased by about 40% from a pre- July 2008 values of -1.0 km^2 to post- July 2008 values of -0.7 to -0.6 km^2 (Figure 15 (top right), blue line). At the same time the meteoric water inventory at Fram Strait rapidly decreased from a July 2008 value of 2.2 km^2 to post July 2008 values of 1.5 to 1.7 km^2 (Figure 15 (top left), red line).

[87] While the 2009–2011 meteoric water inventories are low relative to the long term mean (Figure 14, middle row, left panel and Figure 13), they are not as exceptionally low as the sea ice brine inventories in these years. Rather, a rapid change occurred in the MW:SIM ratio after the July 2008 section (Figure 15, bottom left). The change in the ratio of MW:SIM inventories is mostly driven by the input of meltwater at the surface. Figure 16 shows that deep

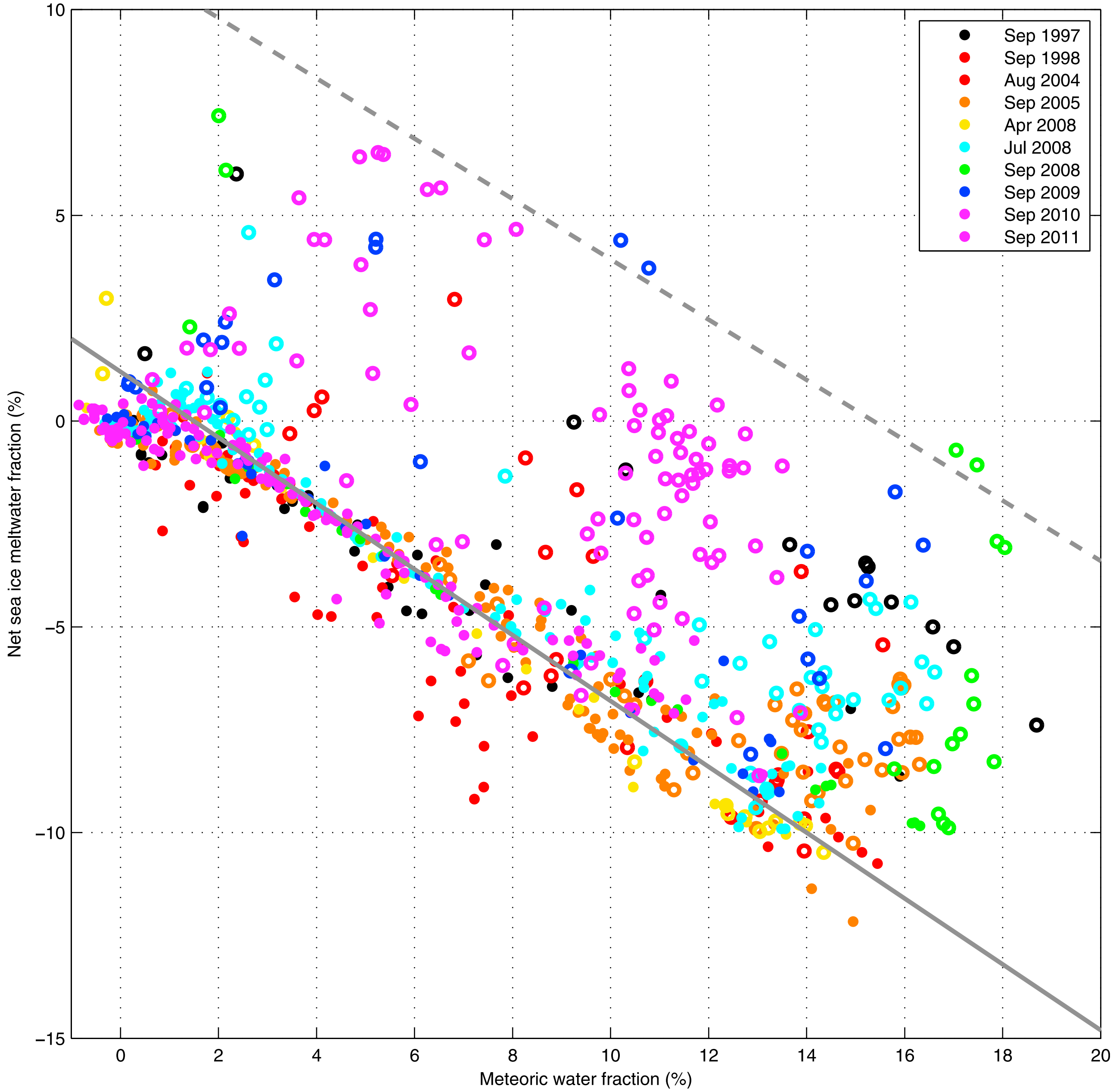

Figure 16. Meteoric water and net sea ice meltwater fraction measurements between 0 and 10 W in Fram strait plotted in meteoric water fraction - sea ice meltwater fraction space. Circles indicate measurements shallower than 25 dbar. Dots indicate measurements deeper than 25 dbar. Solid and dashed grey lines indicate the MW:SIM relationships identified by *Bauch et al.* [2011].

(>25 dbar) samples from the 2009–2011 September sections lie along the same line as samples from previous sections when the meteoric water fraction is plotted against the net sea ice meltwater fraction. However, many surface samples from the 2009–2011 September sections are displaced from this line.

[88] The concurrent rapid reduction of both sea ice brine and meteoric water inventories at Fram Strait after July 2008 suggests that the supply of east Siberian shelf water may have been reduced. However, a reduction in the supply of shelf water does not explain the new recurved shaped of cumulative inventory profiles from 2009 to 2011, nor the change in ratio of MW:SIM inventories. The change in ratio and new profile shape seem to be caused by an increased input of sea ice meltwater at the surface.

6. Summary and Conclusions

[89] We set out to determine if the composition of the Fram Strait freshwater outflow has changed over the last decade. In order to quantify changes we first estimated the long term mean situation in Fram Strait. To avoid bias due to the fact that sections in different years sampled different regions of Fram Strait we consider only the region between

0 and 10 W. Sections that did not span the study region or were not completed in late summer were excluded.

[90] We estimate the 1998–2011 mean late summer inventory of freshwater above 300 dbar and between 0 and 10 W in Fram Strait as follows; meteoric water: 1.8 km^2, equivalent to a mean thickness of 8.5 m; net sea ice meltwater: −0.9 km^2 (−0.9 km^2 brine + 0.03 km^2 meltwater), equivalent to a mean thickness of −4.1 m (−4.2 m brine + 0.1 m meltwater); Pacific freshwater: 0.3 km^2, equivalent to a mean thickness of 1.4 m. Compared with the freshwater budget of *Serreze et al.* [2006] and the modeling study of *Jahn et al.* [2010] we observe a much smaller fraction of Pacific freshwater and a larger fraction of meteoric water. Note that our 1998–2011 mean is weighted to the recent period between 2008–2011 when 5 of the 7 sections were collected.

[91] The freshwater composition determined over the East Greenland shelf was similar to that in the EGC in all sections. No significant freshwater inventories were found east of 0 degrees, therefore the composition determined between 0 and 10 W should be representative of the Arctic Ocean outflow as a whole.

[92] Between 0 and 10 W at Fram Strait the inventory of positive sea ice meltwater is an order of magnitude smaller than the inventory of negative sea ice meltwater (i.e., brine), and was only found between the surface and 25 dbar. We observe large seasonal variations in the inventory of positive sea ice meltwater, with maximum inventories in September sections. Patches of positive sea ice meltwater are found just to the east of the EGC. Although these patches do not amount to a significant inventory in Fram Strait their presence suggests that sea ice can escape from the EGC and melt in the adjacent water. This represents a potential source of freshwater to the Greenland Sea that might be more significant further downstream.

[93] The 1998–2011 mean ratio of meteoric water to net sea ice meltwater inventories between 0 and 10 W was −2:1. The ratio of −2:1 is determined with the benefit of N:P ratio measurements which allow Pacific freshwater to be excluded from meteoric water inventories. If we were to include Pacific freshwater in our meteoric water inventories we would determine a mean ratio of approximately −2.3:1. As there was relatively little Pacific water present in our selected sections, both of these values are close to those determined at Fram Strait by *Bauch et al.* [1995] and *Meredith et al.* [2001], who did not separately identify Pacific freshwater.

[94] The 1998–2011 mean ratio of meteoric water to net sea ice meltwater inventories suggests that relatively more meteoric water (or less sea ice) passes out of Fram Strait relative to the freshwater budget of *Serreze et al.* [2006]. Our comparison with *Serreze et al.* [2006] is based on the assumption that in the long term, the export of sea ice from the Arctic Ocean must be balanced by the export of a corresponding deficit of net sea ice meltwater. However, solid sea ice and sea ice brine do not necessarily follow the same path out of the Arctic Ocean.

[95] Relative to the mean 1998–2011 situation we observe the following changes:

[96] *Large inventories of net sea ice meltwater in 2009, 2010 and 2011.* In 2009 2010 and 2011 we observe the three largest (least negative) inventories of net sea ice meltwater at Fram Strait. These inventories are approximately 30% larger than 1998–2011 mean and 40% larger than comparable pre-2009 inventories. Moreover, the September 2009–2011 sections are the first to show positive fractions of sea ice meltwater at the surface near the core of the EGC close to 5 W.

[97] *Reduced inventories of meteoric water in 2009, 2010 and 2011.* Concurrent with the increased inventories of net sea ice meltwater (decreased inventories of sea ice brine), the September 2009–2011 sections show decreased inventories of meteoric water. The covariance of meteoric water and brine inventories suggests that meteoric water and brine may be delivered to Fram Strait together, possibly from the shelves of the eastern Arctic. This idea is supported by the observation that freshwater outflow at Fram Strait has a similar meteoric water to sea ice meltwater ratio as samples collected in the central Arctic Ocean and Siberian shelves.

[98] *Increased input of sea ice meltwater at the surface in 2009 2010 and 2011.* Sections from September 2009–2011 show an increased input of sea ice meltwater at the surface relative to previous September sections. This suggests that more sea ice now melts back into the surface in late summer than previously. We estimate that the surface meltwater input in recent sections is equivalent to about 10–20% of the net sea ice meltwater inventory. In previous sections there was no significant input at the surface. It is unclear if this melting occurs in Fram Strait or further upstream.

[99] *Return of significant Pacific freshwater inventories in 2011.* Our September 2011 section shows a significant (0.6 km^2) inventory of Pacific freshwater. This is the first time since September 1998 that a significant inventory of Pacific water has been observed in Fram Strait.

[100] *Consistent increase in the amount of sea ice meltwater relative to meteoric water.* From 1998 to 2010, the ratio of meteoric water to net sea ice meltwater inventories decreased with every subsequent section. The ratio of meteoric water to net sea ice meltwater inventories observed in 2011 was higher than the extreme ratios observed in 2009 and 2010, but still indicative of a long term decline.

[101] *Links to the atmospheric circulation.* Changes in the freshwater composition observed in recent Fram Strait sections may be partly linked to the atmospheric circulation. Cyclonic atmospheric circulation anomalies favor the retention of water on the East Siberian shelves [*Proshutinsky and Johnson*, 1997], suggesting that meteoric water and brine inventories at Fram Strait might be reduced after a prolonged cyclonic circulation anomaly.

[102] *Stroeve et al.* [2011] point out that more sea ice is ejected through Fram Strait during cyclonic circulation anomalies, which might increase the amount of surface melting in the vicinity of Fram Strait. Moreover, during anticyclonic circulation anomalies the core of the transpolar drift shifts to the east reducing the flow of older, thicker sea ice from the western Arctic Ocean towards Fram Strait and increasing the flow of younger, thinner sea ice to Fram Strait from the East Siberian Seas [*Proshutinsky and Johnson*, 1997]. Such a change in the source of sea ice could decrease the amount of surface sea ice meltwater input in at Fram Strait because younger, thinner sea ice tends to have a higher salinity than older sea ice and may be less susceptible to melting by ocean heat input.

[103] Further work in this area, will help to clarify if the changes in the freshwater composition observed in recent

sections are indicative of long term change or related to short term variations in the atmospheric circulation.

[104] **Acknowledgments.** Many thanks are due to the officers and crew of the research vessels and to all those who helped us to collect samples from the icy waters of Fram Strait. We wish to thank James Maslanik for helpful discussions regarding the mean age of Arctic sea ice and Rebecca Woodgate for assistance in calculating the mean salinity of the Pacific inflow. We thank Dorothea Bauch and an anonymous reviewer for their comments, which greatly improved the manuscript. P. A. Dodd was funded by the Norwegian Research Council under the IPY project IAOOS-Norway: Closing the loop. B. Rabe was funded by the co-operative project The North Atlantic as Part of the Earth System: From System Comprehension to Analysis of Regional Impacts funded by the German Federal Ministry for Education and Research (BMBF project 03F0605E).

References

Aagard, K., and E. C. Carmack (1989), The role of sea ice and other fresh water in the Arctic circulation, *J. Geophys. Res.*, *94*, 14,485–14,498, doi:10.1029/JC094iC10p14485.

Arzel, O., T. Fichefet, H. Goosse, and J.-L. Dufresne (2008), Causes and impacts of changes in the Arctic freshwater budget during the twentieth and twenty-first centuries in an AOGCM, *Clim. Dyn.*, *30*, 37–58, doi:10.1007/s00382-007-0258-5.

Bauch, D., M. R. van der Loeff, N. Andersen, S. Torres-Valdes, K. Bakker, and E. P. Abrahamsen (2011), Origin of freshwater and polynya water in the Arctic Ocean halocline in summer 2007, *Prog. Oceanogr.*, *91*, 482–495, doi:10.1016/j.pocean.2011.07.017.

Bauch, D. P., P. Schlosser, and R. G. Fairbanks (1995), Freshwater balance and the sources of deep and bottom waters in the Arctic Ocean inferred from the distribution of $H_2^{18}O$, *Prog. Oceanogr.*, *35*, 53–80, doi:10.1016/0079-6611(95)00005-2.

Becker, P. (1995), The effect of Arctic river hydrological cyles on Arctic Ocean circulation, Ph.D. thesis, Old Dominion Univ., Norfolk, Va.

Box, J., D. Bromwich, and L. Bai (2004), Greenland ice sheet surface mass balance 1991–2000: Application of Polar MM5 mesoscale model and in situ data, *J. Geophys. Res.*, *109*, D16105, doi:10.1029/2003JD004451.

Comiso, J. C., C. L. Parkinson, R. Gersten, and L. Stock (2008), Accelerated decline in the Arctic sea ice cover, *Geophys. Res. Lett.*, *35*, L01703, doi:10.1029/2007GL031972.

Cooper, L. W., T. E. Whitledge, J. M. Grebmeier, and T. Weingartner (1997), The nutrient, salinity, and stable oxygen isotope composition of Bering and Chukchi Seas waters in and near the Bering Strait, *J. Geophys. Res.*, *102*, 12,563–12,573, doi:10.1029/97JC00015.

Cooper, L. W., J. W. McClelland, R. M. Holmes, P. A. Raymond, J. J. Gibson, C. K. Guay, and B. J. Peterson (2008), Flow-weighted values of runoff tracers (δ18o, doc, ba, alkalinity) from the six largest Arctic rivers, *Geophys. Res. Lett.*, *35*, L18606, doi:10.1029/2008GL035007.

Dmitrenko, I. A., S. A. Kirillov, H. Eicken, and N. Markova (2005), Wind-driven summer surface hydrography of the eastern Siberian shelf, *Geophys. Res. Lett.*, *32*, L14613, doi:10.1029/2005GL023022.

Dmitrenko, I. A., S. A. Kirillov, and L. B. Tremblay (2008), The long-term and interannual variability of summer fresh water storage over the eastern Siberian shelf: Implications for climatic change, *J. Geophys. Res.*, *113*, C03007, doi:10.1029/2007JC004304.

Dodd, P. A., K. J. Heywood, M. P. Meredith, A. C. Naveira-Garabato, A. D. Marca, and K. K. Falkner (2009), Sources and fate of freshwater exported in the East Greenland Current, *Geophys. Res. Lett.*, *36*, L19608, doi:10.1029/2009GL039663.

Ekwurzel, B. (1998), Circulation and mean residence times in the Arctic Ocean derrived from tritium, helium and oxygen-18 tracers, Ph.D. thesis, Columbia Univ., New York.

Ekwurzel, B., P. Schlosser, R. A. Mortlock, and R. G. Fairbanks (2001), River runoff, sea ice meltwater, and Pacific water distribution and mean residence times in the Arctic Ocean, *J. Geophys. Res.*, *106*, 9075–9092, doi:10.1029/1999JC000024.

Epstein, S., and T. Mayeda (1953), Variations of ^{18}O content of waters from natural sources, *Geochim. Cosmochim. Acta*, *4*, 213–224, doi:10.1016/0016-7037(53)90051-9.

Falck, E., G. Kattner, and G. Budeus (2005), Disapearance of Pacific water in the northwestern Fram Strait, *Geophys. Res. Lett.*, *32*, L14619, doi:10.1029/2005GL023400.

Falck, E., E. P. Jones, G. Kattner, and G. Budeus (2008), Fresh water in the northern East Greenland Current from 1982 through 2005, paper presented at EGU General Assembly, Eur. Geophys. Union, Vienna, Austria.

Giles, K. A., S. W. Laxon, A. L. Ridout, D. J. Wingham, and S. Bacon (2012), Western Arctic Ocean freshwater storage increased by wind-driven spin-up of the Beaufort Gyre, *Nat. Geosci.*, *5*, 194–197, doi:10.1038/NGEO1379.

Gordon, L. I., J. C. Jennings, A. A. Ross, and J. M. Krest (1993), A suggested protocol for continuous flow automated analysis of seawater nutrients (phosphate, nitrate, nitrite and silicic acid) in the WOCE Hydrographic Program and the Joint Global Ocean Fluxes Study, *Methods Manual WHPO 91-1*, WOCE Hydrogr. Program Off., Silver Spring, Md.

Guay, C., K. K. Falkner, R. D. Muench, M. Mensch, M. Frank, and R. Bayer (2001), Wind-driven transport pathways for Eurasian Arctic river discharge, *J. Geophys. Res.*, *106*, 11,469–11,480, doi:10.1029/2000JC000261.

Jahn, A., L. B. Tremblay, R. Newton, M. M. Holland, L. A. Mysak, and I. A. Dmitrenko (2010), A tracer study of the Arctic Ocean's liquid freshwater export variability, *J. Geophys. Res.*, *115*, C07015, doi:10.1029/2009JC005873.

Jones, E. P., L. G. Anderson, and J. H. Swift (1998), Distribution of Atlantic and Pacific waters in the upper Arctic Ocean: Implications for circulation, *Geophys. Res. Lett.*, *25*, 765–768, doi:10.1029/98GL00464.

Jones, E. P., L. G. A. S. Jutterström, L. Mintrop, and J. H. Swift (2008a), Pacific freshwater, river water and sea ice meltwater across Arctic Ocean basins: Results from the 2005 Beringia Expedition, *J. Geophys. Res.*, *113*, C08012, doi:10.1029/2007JC004124.

Jones, E. P., L. G. A. S. Jutterström, and J. H. Swift (2008b), Sources and distribution of freshwater in the East Greenland Current, *Prog. Oceanogr.*, *78*, 37–44, doi:10.1016/j.pocean.2007.06.003.

Kwok, R., G. F. Cunningham, M. Wensnahan, I. Rigor, H. J. Zwally, and D. Yi (2009), Thinning and volume loss of the Arctic Ocean sea ice cover: 2003–2008, *J. Geophys. Res.*, *114*, C07005, doi:10.1029/2009JC005312.

Meredith, M., K. Heywood, P. Dennis, L. Goldson, R. White, E. Fahrbach, U. Schauer, and S. Østerhus (2001), Freshwater fluxes through Fram Strait, *Geophys. Res. Lett.*, *28*, 1615–1618, doi:10.1029/2000GL011992.

New, M., M. Todd, M. Hulme, and P. Jones (2001), Precipitation measurements and trends in the twentieth century, *Int. J. Climatol.*, *21*, 1889–1922, doi:10.1002/joc.680.

Østlund, H. G., and G. Hut (1984), Arctic Ocean water mass balance from isotope data, *J. Geophys. Res.*, *89*, 6373–6381, doi:10.1029/JC089iC04p06373.

Overeem, I., and J. P. M. Syvitski (2010), Shifting discharge peaks in Arctic rivers, 1977–2007, *Geogr. Ann.*, *92*, 285–296, doi:10.1111/j.1468-0459.2010.00395.x.

Parkinson, C. L., and D. J. Calivari (2002), A 21 year record of Arctic sea ice extents and their regional, seasonal and monthly variability and trends, *Ann. Glaciol*, *34*, 441–446, doi:10.3189/172756402781817725.

Parkinson, C. L., D. J. Calivari, P. Gloersen, H. J. Zwally, and J. C. Comiso (1999), Arctic sea ice extents, areas and trends, 1978–1996, *J. Geophys. Res.*, *104*, 20,837–20,856, doi:10.1029/1999JC900082.

Pavlov, V. K., L. A. Timokhov, G. A. Baskakov, M. Y. Kulakov, V. K. Kurazhov, P. V. Pavlov, S. V. Pivovrov, and V. V. Stanovoy (1996), Hydrometerological regime of the Kara, Laptev and East-Siberian Seas, *Tech. Memo. APL-UW TM 1-96*, Appl. Phys. Lab., Univ. of Wash., Seattle.

Peterson, B., R. Holmes, J. McClelland, C. Vorosmarty, R. Lammers, A. Shiklomanov, I. Shiklomanov, and S. Rahmstorf (2002), Increasing river discharge to the Arctic Ocean, *Science*, *298*, 2171–2173, doi:10.1126/science.1077445.

Proshutinsky, A. Y., and M. A. Johnson (1997), Two circulation regimes of the wind-driven Arctic Ocean, *J. Geophys. Res.*, *102*, 12,493–12,514, doi:10.1029/97JC00738.

Rabe, B., U. Schauer, A. Mackensen, M. Karchera, E. Hansen, and A. Beszczynska-Möller (2009), Freshwater components and transports in the Fram Strait: Recent observations and changes since the late 1990s, *Ocean Sci.*, *5*, 219–233, doi:10.5194/osd-6-581-2009.

Rabe, B., M. Karcher, U. Schauer, J. M. Toole, R. A. Krishfield, S. Pisarev, F. Kauker, R. Gerdes, Takashi, and T. Kikuchi (2011), An assessment of Arctic Ocean freshwater content changes from the 1990s to the 2006–2008 period, *Deep Sea Res., Part I*, *58*, 173–185, doi:10.1016/j.dsr.2010.12.002.

Redfield, A. C., B. H. Ketchum, and F. A. Richards (1963), The influence of organisms on the composition of sea-water, in *The Sea: Ideas and Observations on Progress in the Study of the Seas*, pp. 26–77, John Wiley, New York.

Rignot, E., and P. Kanagaratnam (2006), Changes in the velocity structure of the Greenland Ice Sheet, *Nature*, *311*, 986–990, doi:10.1126/science.1121381.

Rudels, B., E. Fahrbach, J. Meincke, G. Budeus, and P. Eriksson (2002), The East Greenland Current and its contribution to Denmark Strait overflow, *ICES J. Mar. Sci.*, *59*, 1133–1154, doi:10.1006/jmsc.2002.1284.

Serreze, M. C., A. P. Barrett, A. G. Slater, R. A. Woodgate, K. Aaraard, R. B. Lammers, M. Steele, R. Moritz, M. Meredith, and C. M. Lee (2006), The large-scale freshwater cycle of the Arctic, *J. Geophys. Res.*, *111*, C11010, doi:10.1029/2005JC003424.

Steele, M., J. Morrison, W. Ermold, I. Rigor, M. Ortmeyer, and K. Shimada (2004), Circulation of summer Pacific halocline water in the Arctic Ocean, *J. Geophys. Res.*, *109*, C02027, doi:10.1029/2003JC002009.

Stroeve, J. C., M. Holland, W. Meier, T. Scambos, and M. Serreze (2007), Arctic sea ice decline: Faster than forecast, *Geophys. Res. Lett.*, *34*, L09501, doi:10.1029/2007GL029703.

Stroeve, J. C., J. Maslanik, M. C. Serreze, I. Rigor, W. Meier, and C. Fowler (2011), Sea ice response to an extreme negative phase of the Arctic Ocsillation during winter 2009/2010, *Geophys. Res. Lett.*, *38*, L02502, doi:10.1029/2010GL045662.

Taylor, J. R., K. K. Falkner, U. Schauer, and M. Meredith (2003), Quantitative considerations of dissolved barium as a tracer in the Arctic Ocean, *J. Geophys. Res.*, *108*(C12), 3374, doi:10.1029/2002JC001635.

Vinje, T., N. Nordlund, and A. Kvarnbekk (1998), Monitoring ice thickness in Fram Strait, *J. Geophys. Res.*, *103*, 10,437–10,449, doi:10.1029/97JC03360.

Wadhams, P., W. B. Tucker, W. B. Krabill, R. N. Swift, J. C. Comiso, and N. R. Davis (1992), Relationship between sea ice freeboard and draft in the Arctic basin, and implications for ice thickness monitoring, *J. Geophys. Res.*, *97*, 20,325–20,334, doi:10.1029/92JC02014.

Woodgate, R. A., and K. Aagard (2005), Revising the Bering Strait freshwater flux into the Arctic Ocean, *Geophys. Res. Lett.*, *32*, L02602, doi:10.1029/2004GL021747.

Wu, P., R. Wood, and P. Stott (2005), Human influence on increasing Arctic river discharges, *Geophys. Res. Lett.*, *32*, L02703, doi:10.1029/2004GL021570.

Yamamoto-Kawai, M., F. A. McLaughlin, E. C. Carmack, S. Nishino, and K. Shimada (2008), Freshwater budget of the Canada Basin, Arctic Ocean from salinity δ^{18}O and nutrients, *J. Geophys. Res.*, *113*, C01007, doi:10.1029/2006JC003858.